International Journal of *Molecular Sciences*

Article

Opuntia ficus-indica (L.) Mill. Extract: From Chemical Characterization to Inflammatory Profiling and Its Potential Effects in a Zebrafish Model of Spinal Cord Injury—A Morphological and Molecular Study

Lidia Pansera [1,2,†], Stefania Pagliari [3,†], Kamel Mhalhel [1,2], Marialuisa Aragona [1,*], Mirea Sicari [1], Mariarosaria Galeano [4], Michele Rosario Colonna [4], Maria Levanti [1], Rosaria Laurà [1], Francesco Abbate [1], Nicola Cicero [5,6], Massimo Labra [3,7], Sepand Rastegar [8], Antonino Germanà [1,*], Luca Campone [3,7,‡] and Giuseppe Montalbano [1,‡]

1 Zebrafish Neuromorphology Lab, Department of Veterinary Sciences, University of Messina, Polo Universitario dell' Annunziata, 98168 Messina, Italy; lipansera@unime.it (L.P.); kmhalhel@unime.it (K.M.); mirea0497@gmail.com (M.S.); mblevanti@unime.it (M.L.); laurar@unime.it (R.L.); abbatef@unime.it (F.A.); gmontalbano@unime.it (G.M.)
2 Department of Chemical, Biological, Pharmaceutical and Environmental Sciences, University of Messina, Viale Ferdinando Stagno D'Alcontres 31, 98166 Messina, Italy
3 Department of Biotechnology and Biosciences, University of Milano-Bicocca, 20126 Milan, Italy; stefania.pagliari@unimib.it (S.P.); massimo.labra@unimib.it (M.L.); luca.campone@unimib.it (L.C.)
4 Department of Human Pathology and Evolutive Age "Gaetano Barresi", University of Messina, Via C. Valeria, 98125 Messina, Italy; mariarosa.galeano@unime.it (M.G.); michelerosario.colonna@unime.it (M.R.C.)
5 Department of Biomedical and Dental Science and Morphofunctional Imaging, University of Messina, 98168 Messina, Italy; nicola.cicero@unime.it
6 Science4life Spin-off Company, University of Messina, Polo Universitario dell' Annunziata, 98168 Messina, Italy
7 NBFC, National Biodiversity Future Center, 90133 Palermo, Italy
8 Institute of Biological and Chemical Systems—Biological Information Processing (IBCS-BIP), Karlsruhe Institute of Technology, 76021 Karlsruhe, Germany; sepand.rastegar@kit.edu
* Correspondence: mlaragona@unime.it (M.A.); antonino.germana@unime.it (A.G.)
† These authors contributed equally to this work.
‡ These authors also contributed equally to this work.

Abstract

Natural compounds are increasingly explored for their ability to modulate multiple molecular pathways involved in inflammation and oxidative stress and for their therapeutic potential. Among these, *Opuntia ficus-indica* (L.) Mill. has attracted growing interest due to its rich phytochemical profile; however, the biological properties of unripe fruits remain largely unexplored. In this study, a hydroalcoholic extract obtained from unripe *O. ficus-indica* fruits was characterized for its chemical composition, antioxidant capacity, and concentration-dependent embryotoxic profile and subsequently investigated in a zebrafish model of spinal cord injury (SCI). UHPLC-HRMS/MS analysis identified 14 secondary metabolites, mainly flavonoids and phenylpropanoid acids. Antioxidant activity was confirmed by DPPH and ABTS assays. An embryotoxicity assessment conducted according to OECD Test Guideline 236 revealed no mortality at concentrations below 100 μg mL^{-1} and an LC_{50} of 323.59 μg mL^{-1} at 96 h post-fertilization, allowing the identification of non-toxic concentrations for subsequent in vivo experiments. Based on these results, the extract was tested in a larval zebrafish SCI transection model. Treated larvae showed improved locomotor recovery, particularly under continuous exposure, accompanied by modulation of molecular pathways involved in inflammation, neurotrophic support, and neurogenesis, including reduced pro-inflammatory cytokine expression and increased BDNF and Sonic Hedgehog signaling markers. Overall, these findings expand current knowledge on unripe

Academic Editor: Gail B. Mahady

Received: 23 December 2025
Revised: 29 January 2026
Accepted: 3 February 2026
Published: 9 February 2026

O. ficus-indica and highlight its potential to modulate molecular pathways involved in SCI-induced damage and repair.

Keywords: *Opuntia ficus-indica*; prickly pear; antioxidants; flavonoids; zebrafish; spinal cord injury; neuroprotection; inflammation

1. Introduction

Spinal cord injury (SCI) represents one of the most severe forms of central nervous system trauma and remains a major clinical challenge due to the lack of effective curative strategies. This condition is characterized by an initial mechanical insult, followed by a cascade of secondary injury processes. The primary injury induces direct cell death, hemorrhage, and the presence of both apoptotic and necrotic neurons and glial cells [1]. The subsequent secondary injury involves the progressive degeneration of the tissue surrounding the necrotic core, thereby amplifying cellular loss and functional impairment [2,3]. This secondary phase is driven by several mechanisms, including the activation of pro-inflammatory cytokines [4,5], which results in inflammation, edema, ischemia, and chronic demyelination at the injury site. The complex pathological environment makes SCI challenging to treat, particularly as oxidative stress and inflammation create a feedback loop that, particularly in mammals, worsens tissue degeneration [6], with the development of glial scars at the wound site, which can inhibit axonal regeneration [7]. Although no definitive cure currently exists, numerous therapeutic approaches, including rehabilitative, cellular, and molecular strategies, have been tested in a variety of animal models. In this context, zebrafish (*Danio rerio*) have emerged as a powerful model for SCI research due to their unique regenerative capabilities, including robust axonal regeneration and neurogenesis, as well as their high genetic and physiological similarity to mammals [8–11]. Adult zebrafish serve as a valuable comparative system for understanding regenerative processes absent in mammals; however, they are often labor-intensive, lack optical transparency, and are unsuitable for large-scale experiments. In contrast, larval zebrafish provide greater experimental versatility, as they are more compatible with the wide array of genetic manipulation techniques and chemical biology approaches available for this species [12]. For this reason, many recent investigations have adopted spinal cord transection models in zebrafish larvae [13–15], where neuronal and axonal regeneration occurs rapidly and can be directly visualized through intravital microscopy. Moreover, these larval models are able to display complex behaviors [16,17] and allow the integration of advanced genetic tools [18] and chemical biology strategies to uncover molecular mechanisms and explore potential therapeutic compounds. Because of these characteristics, zebrafish larvae have become increasingly used for in vivo screening of bioactive compounds. In this framework, natural substances have gained growing interest for their therapeutic potential [19–21]. Among these, flavonoids, a major subclass of polyphenols, exhibit strong antioxidant and anti-inflammatory activities [22–24]. Flavonoids can mitigate secondary damage and support tissue preservation in various pathological conditions, including SCI [9,25,26].

Opuntia ficus-indica (L.) Mill., commonly known as prickly pear, is a member of the Cactaceae family, widely distributed in arid and semi-arid regions of the Americas, the Mediterranean Basin, Africa, and Asia [27]. Beyond its agronomic and ecological relevance, this species has attracted growing interest due to its rich phytochemical profile, including flavonoids, polyphenols, betalains, vitamins, and polysaccharides, which underlie its antioxidant, anti-inflammatory, hypoglycemic, lipid-lowering, and hepatoprotective effects [28–30]. Extracts derived from different plant parts have also demonstrated neuroprotective effects in models of oxidative stress and neurodegeneration [9,31,32]. Despite extensive investigation of cladodes and mature fruits, the biological potential of *O. ficus-indica* unripe fruits remain largely underexplored. In Mediterranean regions such as southern Italy, particularly Sicily, an agricultural practice known as *scozzolatura* [33] involves the removal and disposal of large numbers of unripe fruits to improve the quality of the final harvest, even though they are particularly rich in bioactive compounds such as flavonoids, phenolic acids, and phenylpropanoid acids, representing an underutilized source with promising biomedical and nutraceutical potential. Building on these considerations, the present study aimed to expand current knowledge on the chemical composition of unripe *O. ficus-indica* fruits by identifying compounds with potential biological relevance and to evaluate their effects using zebrafish as an in vivo experimental model of spinal cord injury.

2. Results

2.1. Characterization of Opuntia ficus-indica Extract by UHPLC-HRMS/MS Analysis

To assess the presence of bioactive compounds in the hydroalcoholic extracts of unripe *Opuntia ficus-indica* fruits, a qualitative UHPLC-DAD-HRMS/MS analysis was performed in both positive and negative ionization modes. Given the agreement between the data from both modes, only the negative ion mode was used for compound characterization, and the corresponding chromatographic profile is presented in Figure 1. The analysis revealed the presence of several metabolites, including 14 phenolic compounds, primarily belonging to the subclasses of flavonoids and phenylpropanoic acids, listed in Table 1. Identification was based on retention time, UV/Vis spectra, and MS data (accurate mass and fragmentation patterns), with comparisons to the literature references and spectral databases.

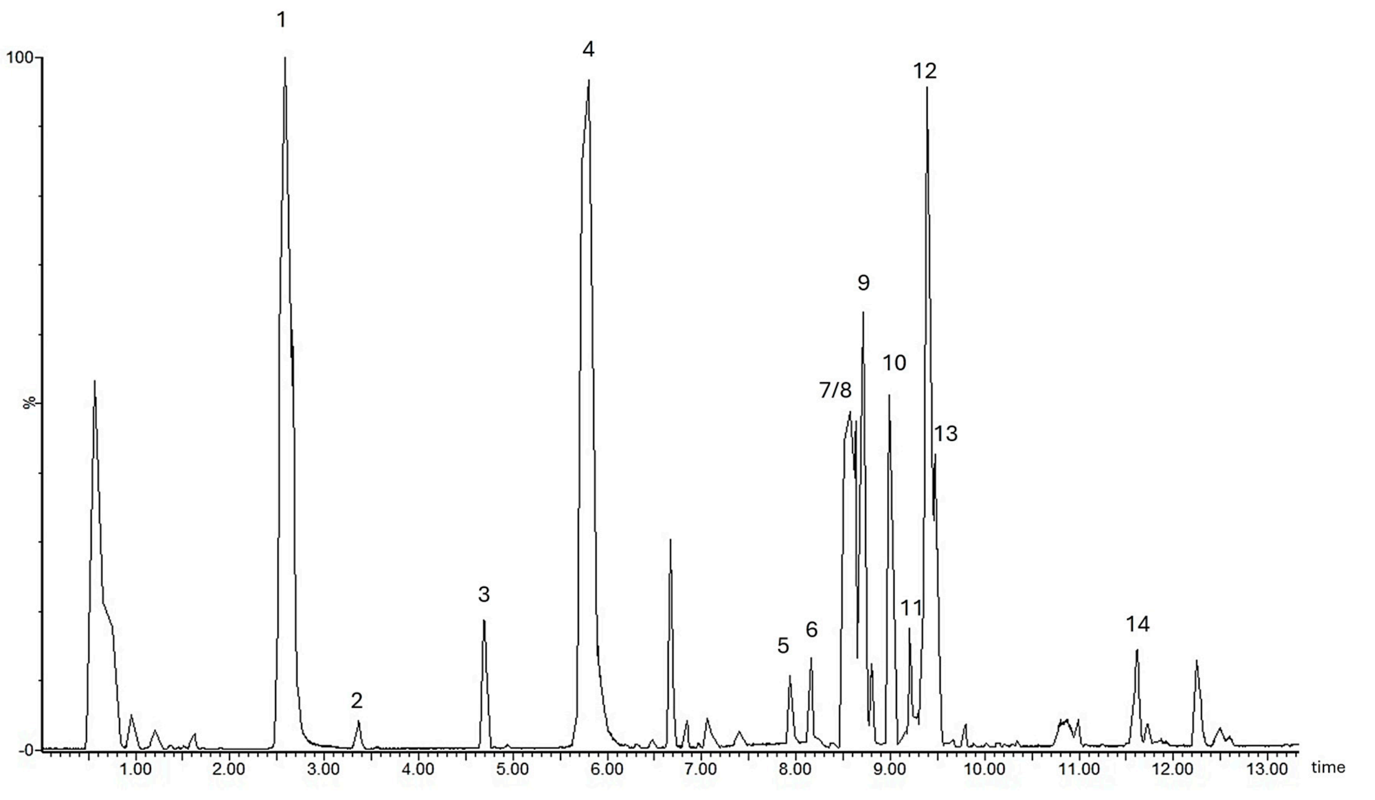

Figure 1. Chromatogram of the chemical profile of *Opuntia ficus-indica* extract acquired by mass spectrometry in negative full ms mode.

Table 1. List of compounds putatively identified by ultrahigh-performance liquid chromatography (UHPLC)-QTOF-high-resolution mass spectrometry (HRMS)/MS analysis.

n	Tr	[M-H]⁻	Neutral Mass	Compound	Class	ppm	Formula	MS/MS	Reference
1	2.58	255.0499	256.0583	Piscidic acid isomer 1	Phenylpropanoic acids	−2.4	$C_{11}H_{12}O_7$	179.0336; 165.0544; 147.0439; 133.0284; 107.0490; 93.0336; 72.9925	[34]
2	3.36	315.0716	316.0795	Protocatechuic acid hexoside	Phenolic acids	0	$C_{13}H_{16}O_9$	152.0102; 108.0205	[35]
3	4.69	255.0499	256.0583	Piscidic acid isomer 2	Phenylpropanoic acids	−2.4	$C_{11}H_{12}O_7$	179.0336; 165.0544; 147.0439; 133.0284; 107.0490; 93.0336; 72.9925	[34]
4	5.80	239.0549	240.0634	Eucomic acid	Phenylpropanoids	−4.2	$C_{11}H_{12}O_6$	179.0545; 149.0595; 107.0489	[35,36]
5	7.94	371.0977	372.1057	Dihydroferulic acid 4-O-glucuronide	Phenolic glycosides	1.8	$C_{16}H_{20}O_{10}$	249.0605; 121.0282; 77.0390	[35]
6	8.16	223.0601	224.0685	2-benzyl-2-hydroxybutanedioic acid	Phenylpropanoic acids	4.9	$C_{11}H_{12}O_5$	161.0595; 133.0651; 117.0697; 91.0543; 87.0084	MS-FINDER
7	8.51	769.2199	770.2271	Isorhamnetin-O-(L-rhamnosyl)-rutinoside	Flavonoid-O-glycosides	−0.3	$C_{34}H_{42}O_{20}$	314.0416; 299.0202	Chemspider
8	8.57	609.1453	610.1535	Rutin	Flavonoid-diglycosides	−0.5	$C_{27}H_{30}O_{16}$	301.0269	[35]
9	8.71	755.2051	756.2114	Isorhamnetin diglycoside isomer	Flavonoid-diglycosides	−1.4	$C_{33}H_{40}O_{20}$	605.1460; 314.0421; 299.0188	[37]
10	8.99	609.1457	610.1535	Rhamnetin hexosyl pentoside	Flavonoid-diglycosides	−0.6	$C_{27}H_{30}O_{16}$	314.042;1 299.0190; 271.0241; 178.9966	[38]
11	9.21	593.1512	594.1585	Kaempferol-ramnosyl glucoside	Flavonoid-diglycosides	−0.1	$C_{27}H_{30}O_{15}$	285.0393	[39]
12	9.39	623.161	624.1691	Isorhamnetin-3-O-rhamnose-7-O-glucoside	Flavonoids-O-glycosides	−1.1	$C_{28}H_{32}O_{16}$	315.0500; 299.0192; 271.0239	[35]
13	9.47	477.1035	478.1112	Isorhamnetin-3-O-hexoside	Flavonoid-3-O-glycosides	−0.8	$C_{22}H_{22}O_{12}$	314.0421; 285.0396; 271.0238; 257.0445; 151.0025	[35]
14	11.61	327.1222	328.1311	Hirsutenone	diarylheptanoid	−3.4	$C_{19}H_{20}O_5$	291.2147; 229.1517; 211.1413; 171.1098	[40]

2.2. Identification of Flavonoids and Phenylpropanoid Acid

Flavonoids are a naturally abundant and heterogeneous class of secondary metabolites characterized by significant antioxidant activity. They are usually present in glycosylated form, i.e., they have one or more sugar fractions attached to the aglycone. There are generally two types of glycosylation (flavonoid C-glycosidic or flavonoid O-glycosidic), which can be distinguished by their characteristic fragmentation patterns. The O-glycosylation pattern is characterized by the neutral loss of 162 Da, 146 Da, and 132 Da, corresponding respectively to the loss of a hexose sugar, a deoxy sugar, and a pentose sugar. In the prickly pear fruit, only O-glycosylated flavonoids were identified. Particularly, compound **13**, with molecular ion m/z 477.1035 $[M\text{-}H]^-$, was assigned the molecular formula $C_{22}H_{22}O_{12}$ based on full-scan acquisition. Given its characteristic MS/MS fragmentation pattern, it was tentatively identified as isorhamnetin O-hexoside. The m/z 315.0621 ion corresponds to the aglycone isorhamnetin, formed by the cleavage of a glycosidic bond and the neutral loss of a hexose sugar (162 Da). The m/z 285.0396 fragment results from the loss of methanol (CH_3OH), attributed to the presence of a methoxyl group in the ortho position on the B-ring. Finally, fragment 151.0025 is related to the cleavage of the bond between C3 and C10 in the C ring of a flavonoid structure, a characteristic fragmentation pattern in this class of compounds. Based on these observations, compounds **7**, **8**, **9**, **10**, **11**, and **12** were identified as isorhamnetin-O-(L-rhamnosyl)-rutinoside, rutin, isorhamnetin diglycoside, rhamnetin hexosyl pentoside, kaempferol-ramnosyl-glucoside, isorhamnetin-O-rhamnose-O-glucoside, and isorhamnetin-O-hexoside. Additionally, compounds **1**, **3**, **4**, and **6** were identified as belonging to the phenylpropanoid acid class, a group of phenolic compounds responsible for high antioxidant activity. In particular, compounds **1** and **3** are two isomers of piscidic acid (m/z 255.0499), based on the specific fragmentation pattern with product ions m/z 179.0336 $[M\text{-}H\text{-}76]^-$ resulting from the loss of glycolic acid and m/z 165.0544 $[M\text{-}H\text{-}90]^-$, resulting from the loss of two carboxylic groups. Compound **4** was identified as eucomic acid (m/z 239.0549) with fragment ion m/z 177.0545 $[M\text{-}H\text{-}62]^-$ due to the loss of one COOH-OH group and m/z 149.0595 $[M\text{-}H\text{-}90]^-$ due to the loss of two carboxyl groups [41].

2.3. In Silico Prediction of Potential Bioactivities of Prickly Pear Extract

The biological potential of the main metabolites identified in prickly pear fruits, thanks to qualitative analysis, was evaluated using the PASS (Prediction of Activity Spectra for Substances) online software tool version 2.0, which predicts the biological activities of substances based on their chemical structures. This software is based on an extensive database of biochemical, pharmacological, and toxicological activities and calculates the probable activity (Pa) and probable inactivity (Pi) values of each compound (Table S1). For the analysis, the SMILES (Simplified Molecular-Input Line-Entry System) strings of each molecule were entered to obtain the respective Pa and Pi values, which show variability in biological activity ranging from 0 to 1. The Pi value must be lower than the Pa value, and the Pa value should be greater than 0.7 for significant reliability.

As shown in Table S1, the results highlight significant antioxidant, antiscavenging, and anti-inflammatory activity for most of the identified compounds. Notably, compounds such as 2-Benzyl-2-hydroxybutanedioic Acid (6), Eucomic acid (4), Isorhamnetin-O-(L-rhamnosyl)-rutinoside (7), and rutin (8) demonstrated high potential for inhibiting enzymes such as NADPH oxidase, NADPH peroxidase, and lipid peroxidase, which play a role in the production of reactive oxygen species (ROS) and lipid peroxides. Furthermore, biocompounds such as Piscidic acid (1,3), Kaempferol-O-glucoside-O-rhamnoside (11), Isorhamnetin 3-rhamnoside-7-glucoside (12), and Isorhamnetin 3-O-glucoside (13) are associated with stabilizing cell membrane integrity. The results were used for preliminary in silico screening to identify the most relevant biological activities and support further experimental investigations.

2.4. Antioxidant Evaluations

The anti-scavenger activity observed in silico was further investigated using two different spectrophotometric assays (DPPH and ABTS) to evaluate the antioxidant capacity of the extracts. The DPPH assay revealed an activity of 0.45 ± 0.039 µmol TE g^{-1} DW (0.11 ± 0.0095 mg TE g^{-1} DW), whereas the ABTS assay showed a higher value of 2.16 ± 0.31 µmol TE g^{-1} DW (0.59 ± 0.085 mg TE g^{-1} DW). These results indicate that the hydroalcoholic extract exhibits a measurable radical scavenging activity, consistently detected by both assays.

2.5. Semi-Quantitative Analysis of Flavonoids and Phenylpropanoid Acid

Given the promising antioxidant activity observed in the spectrophotometric assays, a semi-quantitative analysis of the main identified metabolites was carried out to understand their contribution to the bioactivity. Quantification was performed using UHPLC-UV analysis at 280 nm, employing standard calibration curves. For compounds without available reference standards, quantification was performed using the most structurally analogous standard to obtain the most accurate concentration estimate. Concerning phenolic compounds, the most abundant found in our extract were eucomic acid (compound **4**) with 11,186.21 µg g^{-1} EXT, isorhamnetin-O-rhamnose-O-glucoside (compound **12**) with 4872.92 µg g^{-1} EXT, and isorhamnetin diglycoside (compound **9**) with 3661.16 µg g^{-1} EXT (Table 2).

Table 2. Semiquantitative analysis of the main phenolic acids and flavonoids in *Opuntia ficus-indica* extract.

Compounds	Standard	µg g^{-1} EXT
piscidic acid isomer 1	caffeic acid	6721.29 ± 210.15
piscidic acid isomer 2	caffeic acid	332.05 ± 11.28
eucomic acid	caffeic acid	11,186.21 ± 378.21
isorhamnetin-O-(L-rhamnosyl)-rutinoside	quercetin	2268.77 ± 101.96
rutin	rutin	1976.73 ± 85.04
isorhamnetin diglycoside isomer	quercetin	3661.16 ± 99.16
rhamnetin hexosyl pentoside	quercetin	2645.01 ± 85.97
kaempferol-ramnosyl glucoside	kaempferol	1275.74 ± 79.20
isorhamnetin-3-O-rhamnose-7-O-glucoside	quercetin	4872.92 ± 139.41
isorhamnetin-o-hexoside	quercetin	2088.14 ± 83.52

2.6. Toxicity Evaluation of *Opuntia ficus-indica* Extract on Zebrafish Embryos

ZFET test acceptance criteria were achieved in accordance with OECD guidelines No. 236, as the mortality in the negative control at 96 hpf was 0% and the mortality in the positive control group was 35%. In the positive control group, embryos treated with 4% of 3,4-dichloroaniline (DCA) developed severe yolk sac and cardiac edema (Figure 2).

The mortality rates of zebrafish embryos exposed to different concentrations of *Opuntia ficus-indica* extract (Ofe) were evaluated over a 96-h period. At the highest concentration tested (1600 µg mL^{-1}), 100% mortality was recorded as early as 24 h post-treatment. Similarly, exposure to 800 µg mL^{-1} resulted in 85% mortality after 24 h, rising to 100% by 48 h, with no survivors by the end of the experiment. At a concentration of 400 µg mL^{-1}, a significantly lower mortality rate was observed, with 5% mortality recorded at both 24 and 48 h, which increased to 15% at 72 h and further to 55% by 96 h. Embryos exposed to 200 μg mL^{-1} showed no mortality until the final observation at 96 h, where a slight increase to 5% was recorded. In contrast, concentrations of 100 μg mL^{-1} and below (100, 50, and 25 μg mL^{-1}) did not cause any mortality at any time point (Table 3). The resulting LC50 value at 96 hpf was 323.59 μg mL^{-1}, with BMD confidence interval of 164–370 μg mL^{-1} (Figure 3).

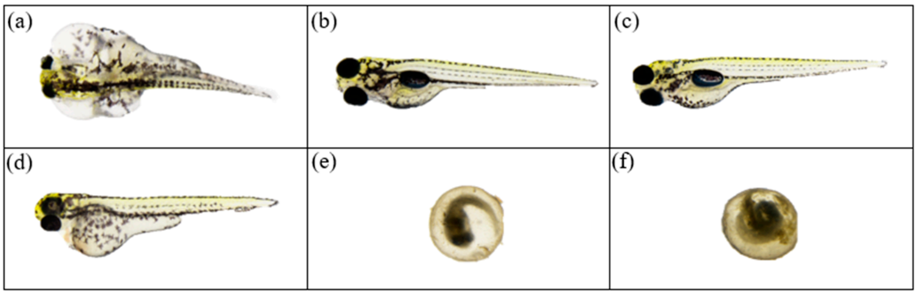

Figure 2. The 96 hpf phenotypes of larvae: (**a**) abnormal phenotype of the 3,4-dichloroaniline (4 μg mL^{-1}) positive control embryo, (**b**) normal phenotype of the negative control (E3 medium), (**c**) normal phenotype of the *Opuntia ficus-indica* extract (Ofe) [25–200 μg mL^{-1}] treated embryo, (**d**–**f**) representative phenotypes of dead embryos treated with 400, 800, and 1600 μg mL^{-1} of Ofe.

Table 3. Mortality rates (%) of zebrafish embryos exposed to *Opuntia ficus-indica* extract (Ofe).

Ofe Concentration (μg mL^{-1})	24 hpf	48 hpf	72 hpf	96 hpf
Ctrl	0%	0%	0%	0%
25	0%	0%	0%	0%
50	0%	0%	0%	0%
100	0%	0%	0%	0%
200	0%	0%	0%	0%
400	5%	5%	15%	55%
800	85%	100%	100%	100%
1600	100%	100%	100%	100%

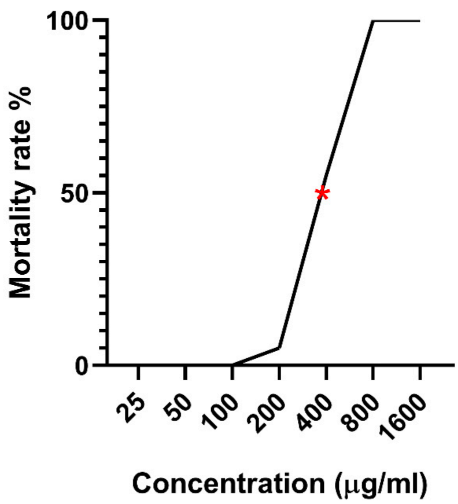

Figure 3. Zebrafish embryo toxicity (ZFET) test. Effect of seven concentrations (25, 50, 100, 200, 400, 800, and 1600 μg mL^{-1}) of Ofe on zebrafish embryo mortality was recorded at 96 h. The asterisk indicates the LC50 value of 323.59 μg mL^{-1}. Values are expressed as a mean ± SD of three independent experiments.

Finally, the effect of the Ofe on hatchings was evaluated during the exposure period. The percentage of the hatching rate was recorded from 48 hpf every 24 h (Table 4). Embryos exposed to concentrations under 200 µg mL^{-1} exhibited hatching rates comparable to the control group. In contrast, exposure to higher concentrations resulted in delayed or failed hatching, observed at 800 and 1600 µg mL^{-1}.

Table 4. Hatching rate (%) of zebrafish embryos exposed to Ofe.

Ofe Concentration (µg mL^{-1})	48 hpf	72 hpf	96 hpf
Ctrl	37.5	91.66667	100%
25	50	100%	100%
50	95	100%	100%
100	65	100%	100%
200	35	95%	100%
400	30	80%	95%
800	0	5%	-
1600	0	-	-

2.7. *Swimming Distance and Velocity Assessments*

The locomotor activity of zebrafish larvae, assessed through swimming distance and velocity, revealed significant differences among the experimental groups, providing insights into the efficacy of the various treatments. Figure 4 presents a detailed analysis of the locomotor behavior of the subjects at 2 days post-injury (dpi), under visible light conditions. Larval movement recordings provided a visual representation of locomotor patterns and activity levels across the experimental groups compared to the Control (Ctrl) group. The Ctrl group exhibited the highest levels of activity, serving as a reference for normal locomotion. The spinal cord injury (SCI) group exhibited a significant reduction in locomotor activity relative to Ctrl groups. In contrast, larvae in the Continuous SCI group (SCI treated with Ofe from 0 to 120 hpf) showed a recovery of motor activity, with an improved velocity and covered distance compared to the SCI group. The Curative SCI group (SCI treated with Ofe after 72 hpf) also demonstrated improved motility, although the effect remained lower than that observed in the Continuous SCI group. Larvae treated continuously and curatively with *Opuntia ficus-indica* extract (Ofe) but not subjected to SCI (Continuous and Curative groups) exhibited locomotor activity and motor performance comparable to those of the Ctrl group (Figure 4a). These findings were further supported by quantitative analysis of the distance traveled and the speed at which the larvae moved over a 120-min observation period (Figure 4b,c). Indeed, significant differences ($p < 0.01$) were observed between the Ctrl and the other five experimental groups, compared to the SCI group, in which the lowest velocity was recorded, indicating the detrimental effects of SCI. Moreover, the Continuous SCI group demonstrated locomotor performance, both in speed and travelled distance, most comparable to the Ctrl group, indicating enhanced functional recovery (Figure 4b,c).

2.8. *Accelerated Healing Across SCI Treatment Groups*

Stereomicroscopic analysis revealed that zebrafish larvae undergoing Continuous SCI and Curative SCI treatment exhibited a higher regenerative response following SCI compared to the baseline physiological regeneration observed in the SCI group (Figure 5h,i,k,m,n,o).

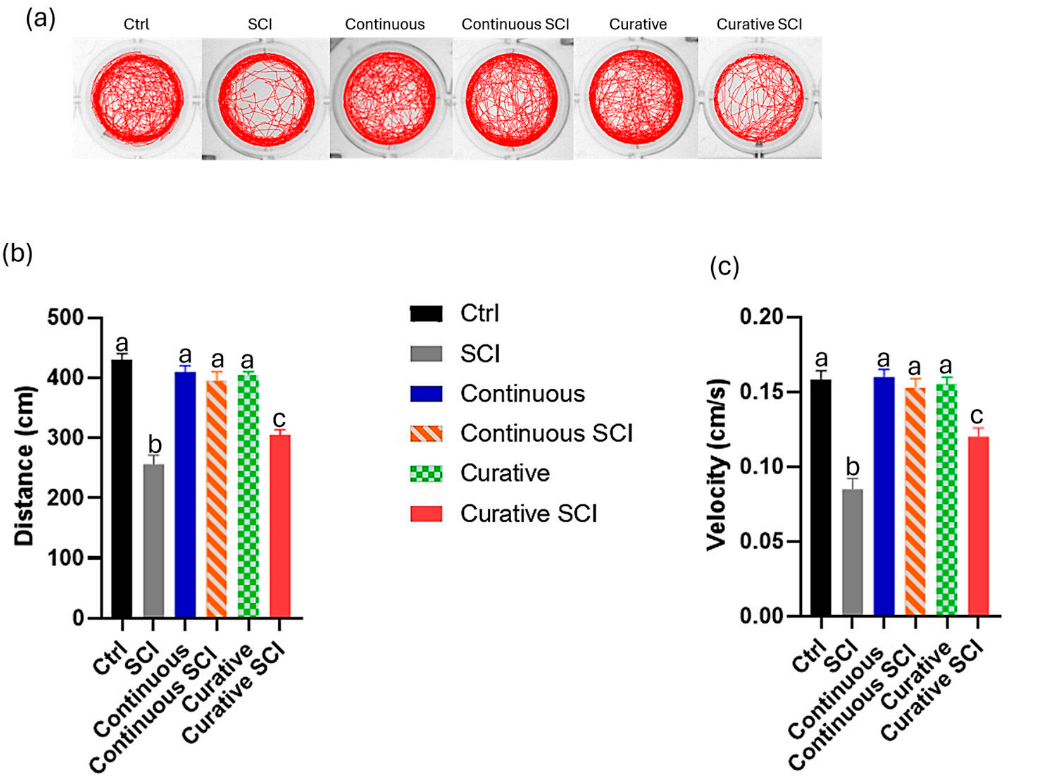

Figure 4. Locomotor behavior assessment in zebrafish larvae across experimental groups (control (Ctrl) group, spinal cord injury (SCI) group, Continuous SCI (SCI treated with Ofe from 0 to 120 hpf) group, Continuous (treatment with Ofe from 0 to 120 hpf without SCI), Curative SCI (SCI treated with Ofe after 72 hpf), Curative groups (treatment with Ofe after 72 hpf without SCI)) at 2 days post-injury. (**a**) Representative records of larval motion trails. (**b**) Free-swimming distance during a 120 min period under visible light conditions (Mann–Whitney U test, $p < 0.05$). (**c**) Free-swimming velocity during the same 120-min period (Mann–Whitney U test, $p < 0.05$). Data are expressed as mean $\pm$ SEM of three replicates. Different lowercase letters (a, b, c) indicate statistically significant differences between the experimental groups.

Following SCI, blood clotting occurs swiftly, effectively halting bleeding almost immediately after the injury induction (T0) (Figure 2a–f). Healing was tracked until 2 dpi. The SCI group showed a progressive closure a few hours after SCI and partial healing by 2 dpi (Figure 2). The Continuous SCI and Curative SCI groups, however, showed notable healing by the second dpi. These findings were expressed within the linear mixed-effects model with Group (SCI, Continuous, Curative), Time (T0, 2 Dpi), and their interaction as fixed effects of the lesion area. It highlighted a significant main effect of Time ($F(1,27) = 6331.177$, $p < 0.001$), indicating a significant reduction in lesion area between T0 and 2 dpi. Moreover, the main effect of the Group × Time interaction was significant ($F(2,27) = 6417$, $p = 0.005$), indicating an effect of the Ofe treatment on lesion evolution over time. The estimated marginal means pairwise comparisons with Bonferroni correction reported a greater reduction in lesion area in both Continuous and Curative SCI groups compared to the SCI group (-1943.100 and -1746.786, respectively, both $p < 0.001$), while no significant difference was observed between the two treated SCI groups (-196.314; $p = 1.000$) (Figure 6).

https://doi.org/10.3390/ijms27041687

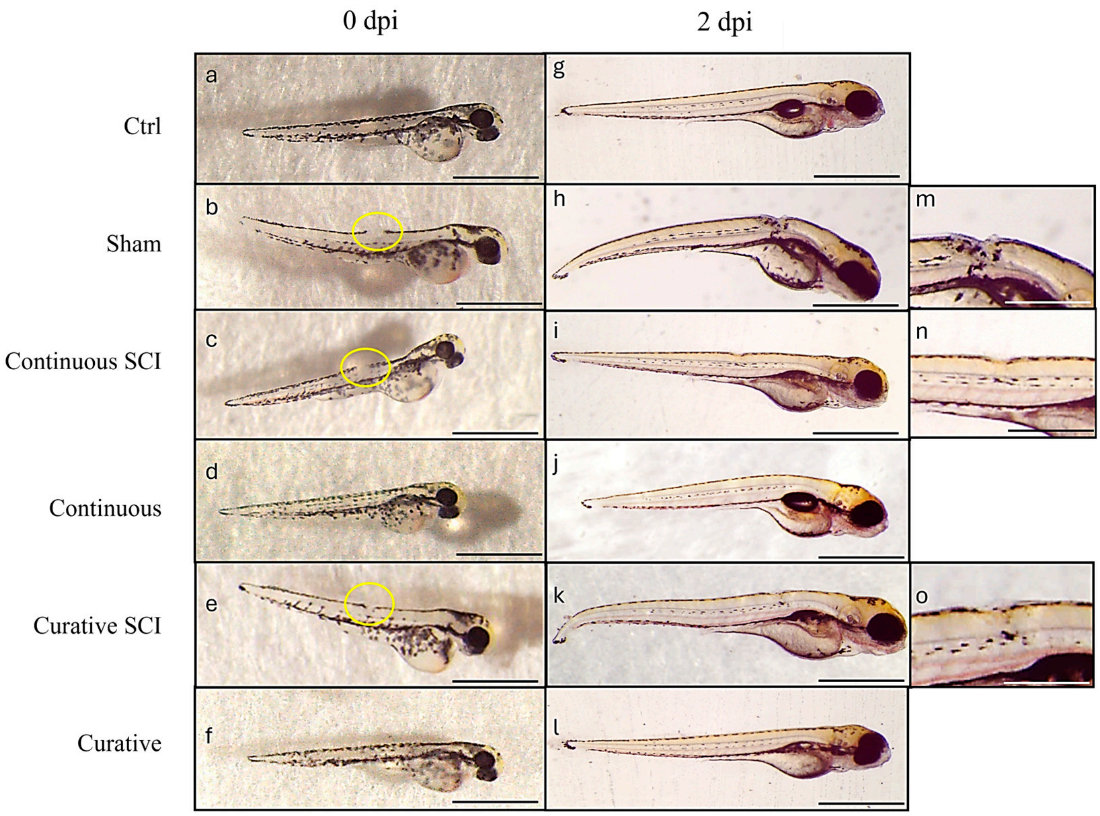

Figure 5. Representative images of zebrafish larvae from the Ctrl, SCI, Continuous SCI, Continuous, Curative SCI, and Curative groups at 0 dpi (**a**–**f**) and 2 dpi (**g**–**l**). Yellow circles (**b**,**c**,**e**) mark the lesion site immediately after injury, while yellow circles (**h**,**i**,**k**,**m**–**o**) indicate the injured area at 2 dpi. Magnification (**a**-**l**) 2.5×; (**m**–**o**) higher magnifications of (**h**,**i**,**k**) respectively. Scale bars: 1 mm (**a**–**l**) and 200 µm (**m**–**o**).

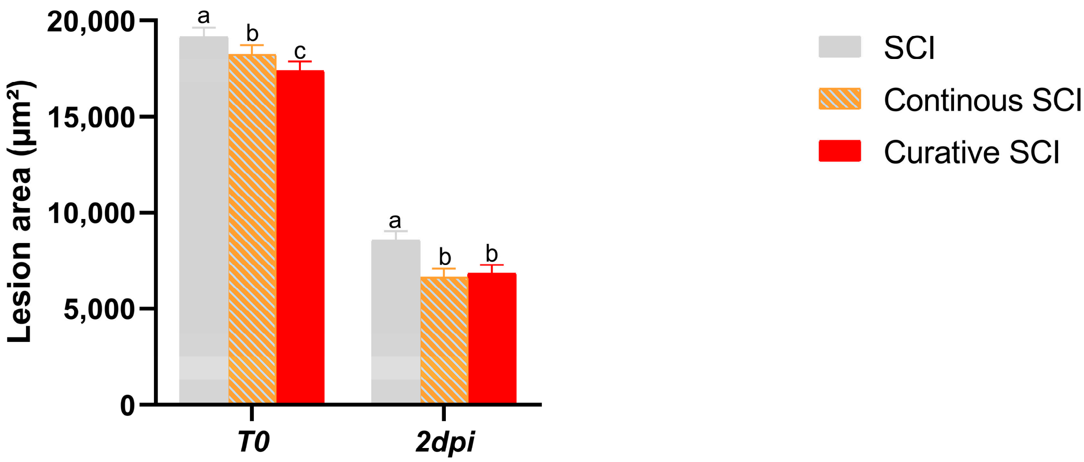

Figure 6. Quantitative analysis of spinal cord lesion area. Estimated marginal means of the lesion area for SCI, Continuous SCI, and Curative SCI groups right after the injury induction (T0) and at 2 days post-injury. Data are presented as estimated marginal means ± SEM derived from the linear mixed-effects model. Statistically significant differences, within each time point, indicated by different letters (a, b, and c), were assessed by post-hoc pairwise comparisons with Bonferroni correction ($p < 0.05$). Bars sharing at least one letter are not significantly different; bars with no letters in common differ significantly.

2.9. Inflammatory Markers Assay: IL-1β, IL-8, TNF-α

In the present work, the expression levels of the pro-inflammatory cytokines IL-1β, IL-8, and TNF-α were assessed across the experimental groups: Ctrl, SCI, Continuous SCI, Curative SCI, Continuous, and Curative. One-way ANOVA revealed a significant effect of group for all three cytokines (IL-1β: $F(5,18) = 1182.84$, $p < 0.001$; IL-8: Welch's $F(5, 8.19) = 413.35$, $p < 0.001$; TNF-α: $F(5,18) = 608.30$, $p < 0.001$).

Post hoc analyses showed that the SCI group showed the highest level of expression for all three markers (all $p < 0.01$). Both the Continuous SCI and Curative SCI treatment groups demonstrated a substantial reduction in the levels of IL-1β, IL-8, and TNF-α, compared to the SCI group (all $p < 0.001$ and all $p < 0.01$, respectively), with inflammatory cytokine levels significantly higher in Curative SCI than Continuous SCI (all $p < 0.05$), except for the IL-8 ($p = 0.001$) group. Finally, groups treated continuously did not differ from Ctrl for IL-8 ($p = 0.238$) or TNF-α ($p = 0.995$), but exhibited a small yet statistically significant increase in IL-1β expression compared with Ctrl ($p < 0.001$). The Curative group, however, did not differ significantly from the Ctrl group for any of the cytokines (IL-1β: $p = 0.324$; IL-8: $p = 0.233$; TNF-α: $p = 0.097$) (Figure 7).

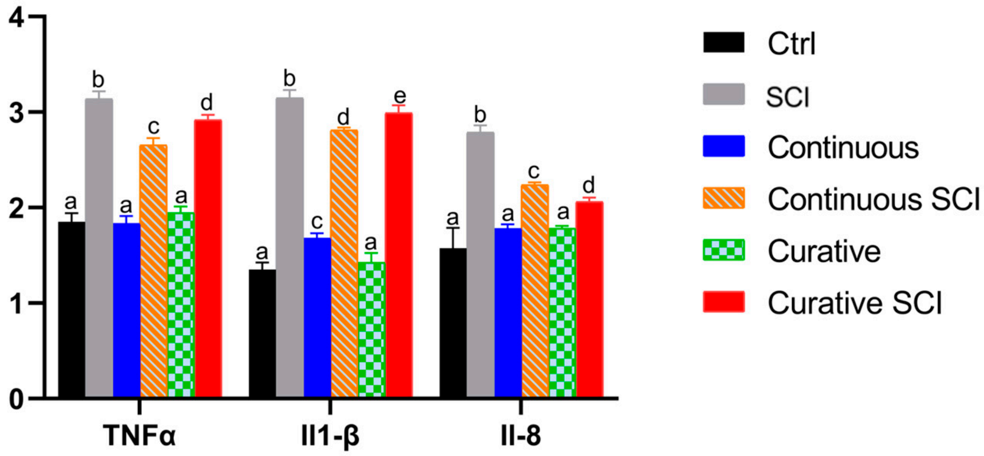

Figure 7. mRNA expression of inflammatory cytokines (IL-1β, IL-8, TNF-α) in different experimental groups (Ctrl, SCI, Continuous SCI, Continuous, Curative SCI, Curative). Data are presented as mean ± SD. Significant differences are indicated by different letters (a, b, c, d, e) on the bars, with lowercase letters indicating significant differences between treatment groups, as determined by one-way ANOVA and Tukey HSD for IL-1beta and TNF alpha, and ANOVA's Welch test with Games–Howell post hoc test for IL-8.

2.10. Neurotrophic Factor Expression

The expression of brain-derived neurotrophic factor (BDNF) was analyzed to investigate its role in modulating spinal cord repair processes following traumatic injury in zebrafish larvae. A one-way ANOVA revealed a significant variation among the experimental groups, $F(5, 18) = 2367.47$, $p < 0.001$, $\eta^2 = 0.998$, with an extremely large effect size. Post hoc comparisons using Tukey's HSD test showed that the Ctrl group exhibited the baseline levels of BDNF expression. The spinal cord injury (SCI) group showed a slightly higher mean BDNF expression than Ctrl; however, this difference was not statistically significant ($p = 0.472$). In contrast, all groups treated with *Opuntia ficus-indica* extract (Ofe), both in the presence and absence of injury, displayed significantly higher BDNF expression compared to Ctrl (all $p < 0.001$).

Among injured larvae groups, the Continuous SCI group exhibited significantly higher BDNF expression than the Curative SCI group ($p = 0.001$). Finally, the groups that received

Continuous or Curative treatment with Ofe in the absence of SCI showed BDNF expression levels higher compared to the Ctrl group (all $p < 0.001$) (Figure 8).

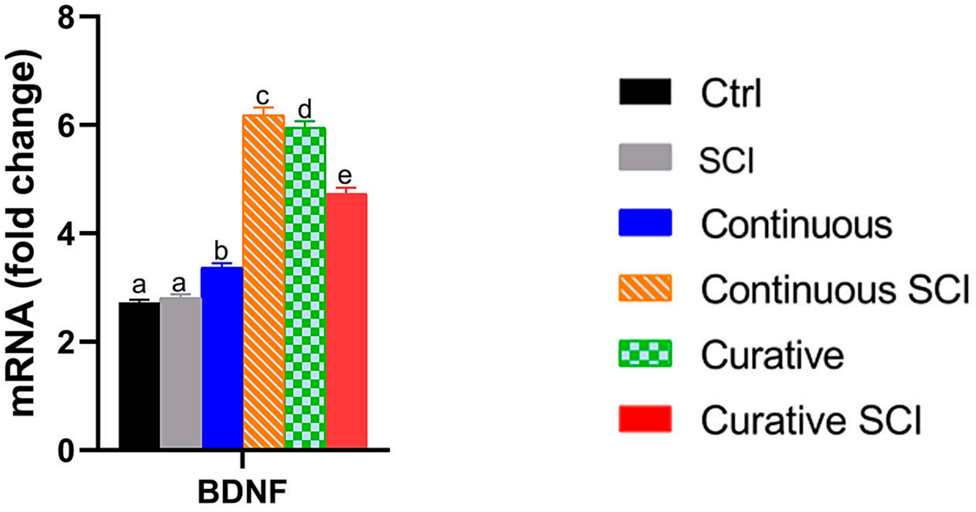

Figure 8. BDNF mRNA expression in different experimental groups (Ctrl, SCI, Continuous SCI, Continuous, Curative SCI, Curative groups). Data are expressed as mean ± SD. One-way ANOVA and Tukey HSD were conducted. Letters (a, b, c, d, e) indicate statistically significant differences between groups ($p < 0.05$).

2.11. Analysis of Sonic Hedgehog-Related Gene Expression

In the present study, the expression of *shh*, *nestin*, and *ngn1*, key genes involved in the Sonic Hedgehog signaling pathway, was evaluated in zebrafish larvae subjected to SCI and treated with Ofe. One-way ANOVA revealed a significant effect of treatment group on shh expression, $F(5, 18) = 780.62$, $p < 0.001$, $\eta^2 = 0.995$. A significant group effect was also observed for ngn1 expression, $F(5, 18) = 295.01$, $p < 0.001$, $\eta^2 = 0.988$, and for nestin expression, $F(5, 18) = 198.99$, $p < 0.001$, $\eta^2 = 0.982$. Since the homogeneity of variance has been violated for all three genes (all $p < 0.05$), robust Welch tests were also conducted and confirmed significant group differences for shh, $F(5, 8.12) = 12{,}444.20$, $p < 0.001$, ngn1, $F(5, 8.22) = 4207.39$, $p < 0.001$, and nestin, $F(5, 8.00) = 4497.21$, $p < 0.001$.

Post hoc comparisons (Games–Howell) revealed that SCI alone significantly altered gene expression compared to Ctrl (SCI vs. Ctrl, all $p < 0.05$). Continuous Ofe treatment significantly increased the expression of shh, ngn1, and nestin in injured larvae (Continuous SCI) compared with untreated injured larvae (SCI vs. Continuous SCI, all $p \leq 0.011$). Curative Ofe treatment administered after injury (Curative SCI) also significantly increased shh, nestin, and ngn1 expression compared with SCI alone (SCI vs. Curative SCI, all $p < 0.05$).

When comparing treatment timing under injury conditions, Continuous SCI showed significantly higher expression levels of shh and ngn1 than Curative SCI (both $p < 0.05$), whereas no significant difference was observed for nestin ($p > 0.05$). In non-injured larvae, Ofe exposure significantly increased nestin expression under both Continuous and Curative regimens (both $p < 0.001$), whereas shh and ngn1 differed from Ctrl only in the Curative group ($p < 0.001$ and $p = 0.041$, respectively), with no significant differences between Ctrl and the Continuous group ($p = 0.104$ and $p = 0.119$), confirming a biological activity of the extract independent of injury (Figure 9).

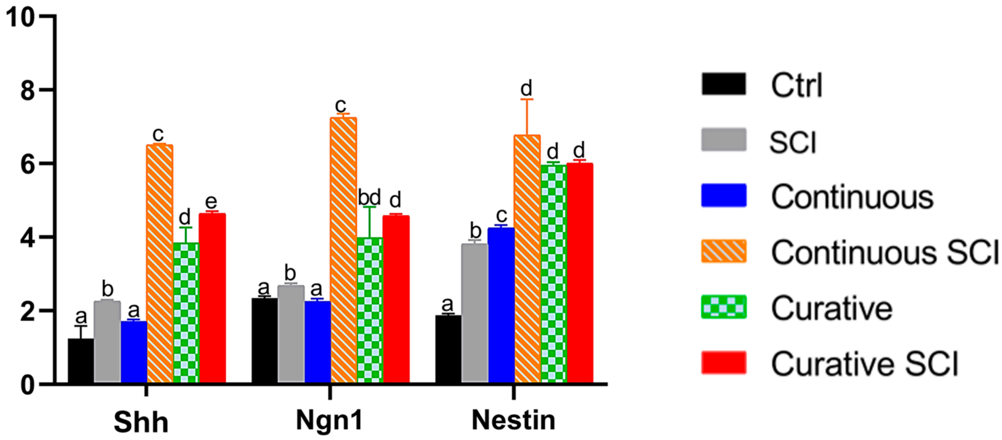

Figure 9. *Shh, Nestin,* and *Ngn1* mRNA expression in different experimental groups (Ctrl, SCI, Continuous SCI, Continuous, Curative SCI, Curative groups). Data are expressed as mean ± SD from three independent experiments. Statistical significance was assessed using ANOVA's Welch with Games–Howell post hoc test. Letters (a, b, c, d, e) indicate statistically significant differences between groups ($p < 0.05$).

3. Discussion

The characterization of plant-derived products is increasingly relevant because many species contain secondary metabolites with potential biomedical applications. However, translating natural compounds into credible health-oriented evidence requires rigorous, integrated workflows combining chemical profiling with biological and toxicological validation. In this framework, fruit and vegetable by-products (e.g., peels, leaves, seeds) are widely recognized as reservoirs of antioxidant and anti-inflammatory metabolites [42,43].

Opuntia ficus-indica represents a promising source of bioactive secondary metabolites, with antioxidant and anti-inflammatory properties [44] that have been investigated mainly in the mature fruit [19,45,46]. By contrast, the unripe fruit remains comparatively underexplored despite its potential as a rich phytochemical matrix; therefore, detailed chemical characterization is essential to expand current knowledge and to support mechanistic links between composition and biological activity.

In the present study, we characterized a hydroalcoholic extract from unripe *O. ficus-indica* fruit by UHPLC-HRMS/MS, quantified its major metabolites, assessed antioxidant capacity using DPPH and ABTS assays, and evaluated its safety profile by estimating LC50 in zebrafish embryo screening. We then investigated the effects of the *Oputia ficus-indica* extract (Ofe) in a zebrafish larval spinal cord injury (SCI) model, focusing on inflammatory and neuroprotection-related markers as well as functional recovery. Overall, our results indicate that continuous exposure to Ofe is associated with more consistent molecular and behavioral benefits than shorter or delayed regimens. Notably, comparing Continuous (0–120 hpf, no SCI) and Curative (post-72 hpf, no SCI) paradigms revealed distinct recovery signatures, suggesting that the timing and duration of administration critically shape efficacy. In this framework, the present study provides experimental evidence linking the phytochemical profile of unripe *O. ficus-indica* to the modulation of inflammatory and neurogenic pathways in vivo.

3.1. Qualitative Analysis of Hydroalcoholic Opuntia ficus-indica Fruit Extract

The UHPLC-HRMS/MS characterization of the hydroalcoholic extract revealed the presence of 13 phenolic compounds, mainly belonging to flavonoids and phenylpropanoic acids, the primary phenolic constituents in the unripe fruit, highlighting the rich phytochemical composition of this cactus fruit. Such findings are consistent with previous studies reporting the presence of bioactive phenolic constituents in various parts of *Opuntia ficus-indica*, including the cladodes, flowers, and ripe fruits [35,47,48]. This chemical profile is consistent with previous studies on *O. ficus-indica*, where compounds such as piscidic acid, eucomic acid, rutin, kaempferol glycosides, and isorhamnetin derivatives are often described [49], and flavonoid glycosides, including isorhamnetin and kaempferol derivatives, are recurrently reported in *Opuntia* fruit and peel analyses [50]. Notably, no non-glycosylated flavonoids were detected, which aligns with previous reports indicating that glycosylation is a prevalent modification in *O. ficus-indica* fruits, enhancing the stability, solubility, and bioavailability of flavonoid molecules [51–53].

Unlike data obtained from mature fruits, where piscidic acid is often reported as the dominant phenolic metabolite [54], the extract analyzed in the current study exhibited a broader distribution of phenolic classes. This suggests a dynamic shift in secondary metabolite biosynthesis during fruit maturation. The dominance of phenolic acids and flavonoids in the unripe stage may indicate a defensive role against environmental stressors, which could decline as the fruit matures and focuses on pigment production to attract seed dispersers [55–57]. Some of the compounds detected, such as isorhamnetin and kaempferol derivatives, occur in O-glycosylated forms, a structural feature that confers improved solubility, stability, bioactivity, bioavailability, compartmentalization, and overall biological activity of phenylpropanoids, thereby enhancing their functional potential [58–60]. Moreover, most of these metabolites are well recognized for their antioxidant and protective properties [58,61–63]. The presence of these bioactive compounds provides a mechanistic explanation for the radical scavenging activity observed in vitro.

The absence of a comparison between unripe and ripe fruit extracts made and tested under identical conditions is one of the limitations of the current study. Given the known maturation-dependent remodeling of secondary metabolism, future studies will directly compare phytochemical fingerprints and in vivo efficacy across fruit stages to identify the maturity window differential production of constituents contributing to the above-observed effects.

3.2. In Silico Predictions and In Vitro Antioxidant Activity of Unripe Opuntia ficus-indica Extract

To provide a mechanistic framework for the experimental antioxidant findings, the biological activities of the identified phytochemicals were first explored using in silico prediction. PASS analysis suggested that several compounds present in the unripe *Opuntia ficus-indica* hydroalcoholic extract are potentially associated with antioxidant- and inflammation-related activities, including free radical scavenging, lipid peroxidase inhibition, modulation of NADPH oxidase and peroxidase activities, and preservation of membrane integrity ($Pa > Pi$ for these activities). PASS-based approaches are widely employed in phytochemical and natural product research to predict probable biological activities on the basis of molecular structure and to guide the interpretation of subsequent experimental assays, with predicted activities discussed as probabilistic indications rather than direct experimental evidence [64–66]. In line with previous studies integrating PASS predictions with in vitro antioxidant assays, high Pa values for membrane integrity agonism and ROS-related enzyme modulation have been interpreted as supportive of antioxidant and anti-inflammatory mechanisms, particularly for polyphenol- and flavonoid-rich extracts [67]. Notably, the recurrent prediction of membrane integrity preservation across multiple metabolites is of particular relevance, as membrane protection is tightly associated with antioxidant and anti-inflammatory responses by limiting lipid peroxidation, reducing oxidative damage, and attenuating the activation of secondary inflammatory cascades, as widely documented for polyphenols and flavonoid-based compounds in oxidative and inflammatory contexts [6,68–70]. Consistent with the in silico predictions, the radical scavenging activity experimentally measured for the unripe *Opuntia ficus-indica* extract falls within the broad range of antioxidant values reported for different prickly pear matrices, although direct quantitative comparison is limited by differences in fruit maturity, extraction procedures, and data normalization. Monter-Arciniega et al. (2019) reported an antioxidant capacity of 1485.14 µmol TE/100 g DW using the ABTS assay, while Marhri et al. (2024) described DPPH and ABTS values of 1.19 mg TE g^{-1} DW and 0.30 mg TE g^{-1} DW, respectively, in prickly pear peels [71,72]. In the present study, the hydroalcoholic extract from unripe fruits exhibited DPPH values of 0.45 ± 0.039 µmol TE g^{-1} DW (0.11 ± 0.0095 mg TE g^{-1} DW) and ABTS values of 2.16 ± 0.31 µmol TE g^{-1} DW (0.59 ± 0.085 mg TE g^{-1} DW), indicating a measurable antioxidant capacity despite differences in matrix composition and developmental stage.

3.3. Semi-Quantitative Analysis of the Main Phenol Compounds

The semi-quantitative analysis revealed eucomic and piscidic acid as the most abundant compounds within the phenylpropanoid acid subclass, both commonly occurring in *O. ficus-indica* plants. The concentrations observed in this study were lower than those reported by Zeghbib et al. [73], in which the authors have reported 47,716.52 ± 1840.45 µg g^{-1} EXT for eucomic acid and 9896 µg g^{-1} EXT for piscidic acid in the fruit flesh [73]. However, the levels of eucomic and piscidic acids found in this extract were higher than those found in the hydroalcoholic extract (80% EtOH) of *O. ficus-indica* var. giallo, which contained 1.061 ± 0.04 mg g^{-1} EXT of piscidic acid and 1.40 ± 0.01 mg g^{-1} EXT of eucomic acid [74]. Additionally, the most abundant metabolites detected among flavonoids were the glycosylated derivatives isorhamnetin-O-rhamnose-O-glucoside and kaempferol-3-gentiobioside-7-rhamnoside. The high content of isorhamnetin-O-rhamnose-O-glucoside, which in our extract exceeded the concentrations reported for the fruits of *O. ficus-indica* var. giallo (0.77 mg g^{-1} EXT) and *O. ficus-indica* var. sanguinosa (1.77 mg g^{-1} EXT) [74]. This observation reinforces the hypothesis that flavonoid glycosides are key constituents of the phytochemical profile of prickly pear fruits and likely play a pivotal role in mediating their documented bioactive properties.

3.4. Toxicological Assessment

Zebrafish embryo toxicity testing (ZFET) complemented the chemical and functional data by defining concentration ranges suitable for future applications. This screening model offers several advantages, such as large sample sizes, low costs, the ability to test dozens to hundreds of phytochemicals rapidly for toxicity assessment, bioactivity screening, phenotypic effects, and ease of handling [9,17,75,76]. In the present work, OECD acceptance criteria were fully met, confirming the validity of the ZFET assay. The absence of mortality in the negative control demonstrated embryo stability under standard conditions, whereas the positive control (DCA) induced the expected severe yolk sac and cardiac edema, consistent with the oxidative stress and increased ROS (reactive oxygen species) production previously reported for this compound [77]. Moreover, DCA treatment caused alterations in mobility, including an impaired escape response, further validating the toxicological reliability of the assay. Exposure to the hydroalcoholic extract of *Opuntia ficus-indica* showed a clear concentration-dependent toxicity profile, with higher concentrations (800 and 1600 µg mL^{-1}) being highly toxic, while lower concentrations of 100 µg mL^{-1} and below (100, 50, and 25 µg mL^{-1}) did not result in any observable mortality at any time point, indicating that these lower concentrations were not acutely toxic to the embryos within the 96-h exposure period.

These findings are consistent with previous studies investigating plant-derived extracts in zebrafish, which have similarly identified non-toxic concentration ranges suitable for subsequent biological testing [17,78,79]. The definition of a safe threshold ($\leq$100 µg mL^{-1} in this case) provides a solid basis for future in vivo and in vitro investigations, supporting the potential use of *O. ficus-indica* extract in nutraceutical research while ensuring toxicological safety. Still, it is important to note that the effective concentrations identified in this study may not directly translate to higher vertebrates or humans due to interspecies differences in physiology, metabolism, and bioavailability.

3.5. Behavioral Evaluation and Stereomicroscopic Observation of Regenerative Effects in Spinal Cord Injury

The locomotor activity of zebrafish larvae, assessed through covered swimming distance and velocity, revealed significant differences among the experimental groups, providing insights into the efficacy of the various treatments. These parameters have been a assessedunder continuous light condition in accordance with various studies [80,81], while other experimental protocols have evaluated similar parameters using light–dark cycles [82]. While the spinal cord injury (SCI) group exhibited a marked reduction in locomotor capacity, among the treatment groups, statistical analysis revealed that the Continuous SCI (SCI treated with Ofe from 0 to 120 hpf) group achieved the most significant recovery compared to others, with locomotor activity metrics closely matching those of the control (Ctrl) group. Conversely, the Curative SCI (SCI treated with Ofe after 72 hpf) group showed modest recovery, with locomotor activity remaining significantly reduced compared to the Continuous SCI group, reflecting the limited potential for repair when intervention is delayed. These results underscore the importance of treatment, timing, and consistency, with continuous therapeutic strategies emerging as the most effective for restoring locomotor activity. Moreover, larvae continuously and curatively treated with *Opuntia ficus-indica* extract (Ofe) in the absence of SCI showed locomotor ability levels comparable to those observed in the Ctrl group, suggesting that the Ofe, in the absence of injury, does not impair normal motor function. Statistical analysis also highlights the significance of these differences. These findings indicate that Ofe has the potential to promote spinal cord regeneration and improve locomotor function in zebrafish larvae, with continuous treatments yielding the most pronounced effects. Furthermore, stereomicroscopic observations were conducted at 0 and 2 days post-injury (dpi) to monitor the progression of tissue recovery. Zebrafish larvae are well known for their intrinsic capacity to regenerate the spinal cord, achieving axonal bridging and functional recovery within a few days post-injury, primarily through activation of pro-regenerative glial cells [83–85]. However, our monitoring showed reduced tissue disruption at the lesion site in the treated groups (Continuous SCI and Curative SCI) compared to the untreated SCI group. In the latter, structural damage remained evident at 2 dpi, indicating a slower resolution of injury-related alterations. These findings parallel previous reports where plant-derived extracts enhanced both structural and functional recovery following SCI in mammalian models. *Lavandula angustifolia* extract, for example, improved locomotor performance, reduced cavity size, preserved ventral motor neurons, and decreased astrogliosis in rat contusion SCI [86]. Icariin promoted histologically verified tissue repair and myelin preservation while improving gait and locomotor scores, partly by suppressing glial scar formation via YAP pathway inhibition [87]. Overall, the above-mentioned evidence supports the predicted Ofe potential likely exercised through its neuroprotective and anti-inflammatory phenolic compounds, probably accelerating the healing of injury and promoting earlier structural restoration, complementing the intrinsic regenerative processes of the zebrafish spinal cord.

3.6. Inflammatory Cytokine Profiling: IL-1β, IL-8, and TNF-α

Following SCI, an inflammatory response is triggered, characterized by a significant increase in leukocytes and pro-inflammatory cytokines, including interleukin-1 beta (IL-1β), interleukin-8 (IL-8), and tumor necrosis factor-alpha (TNF-α) [88,89]. This process facilitates the infiltration of leukocytes into the injury site, exacerbating tissue damage. Although the interactions between inflammation and mitochondrial function remain incompletely understood, the elevated production of inflammatory cytokines following SCI may contribute to the onset of neurological impairments associated with secondary damage [90]. In the present work, the expression levels of the pro-inflammatory cytokines IL-1β, IL-8, and TNF-α were assessed across different experimental groups: Ctrl, SCI, Continuous SCI, Continuous, Curative SCI, and Curative. The SCI group exhibited significantly higher expression levels of pro-inflammatory cytokines compared to the Ctrl group and the other experimental groups treated with Ofe, indicative of the notable inflammation associated with SCI in zebrafish larvae. Larvae treated with Ofe either continuously or curatively (Continuous and Curative groups) exhibited lower expression of IL-1β, IL-8, and TNF-α compared to the SCI group and were more similar to the Ctrl group. Notably, in the Continuous SCI group, a significant reduction of IL-1β, IL-8, and TNF-α expression was observed compared to both the other two groups affected by SCI (SCI and Curative SCI groups). This suggests that treatment with Ofe throughout the entire experimental period (from 0 to 120 hpf), both before and after SCI, enhances the anti-inflammatory response more effectively than post-lesion treatment alone. These findings imply that preventive administration of the extract potentiates the organism's resilience to injury. This evidence aligns with existing research in vitro and in vivo demonstrating that *O. ficus-indica*-derived phenolic compounds, including quercetin and isorhamnetin derivatives, have the capacity to modulate inflammatory processes by reducing the transcription of pro-inflammatory mediators such as TNF-α and IL-1β [91,92]. Additionally, the plant's methanolic flower extracts have shown anti-inflammatory efficacy comparable to indomethacin in reducing paw edema, underscoring its potential as a natural anti-inflammatory agent [93]. Furthermore, flavonoids are known to influence the key pathways of inflammation and tissue damage in SCI [94,95]. The lack of significant differences between the Continuous SCI groups and the Curative SCI group indicates that ongoing administration of the treatment maintains its anti-inflammatory effects more consistently and for longer than a single, curative intervention. These Ofe anti-inflammatory properties likely contribute to enhanced tissue integrity and reduced cytokine expression observed in the Continuous SCI group. The Curative SCI group, despite showing some benefit, had higher inflammatory marker levels than the Continuous SCI group, which could suggest that the bioactive compounds in Ofe may require consistent exposure to maintain optimal modulation of inflammatory pathways. This aligns with findings from studies on neurodegenerative conditions, where earlier intervention leads to better outcomes [96]. In conclusion, the Continuous SCI treatment, likely due to the sustained presence of anti-inflammatory compounds such as flavonoids, demonstrates the greatest potential for modulating inflammation and promoting recovery following spinal cord injury in zebrafish larvae.

3.7. BDNF mRNA Levels Reflect Neuroregenerative Response to Treatment

Brain-derived neurotrophic factor (BDNF) is a member of the neurotrophin family that plays a crucial role in modulating repair processes following traumatic events [97–99]. It supports neuronal survival, development, and synaptic plasticity [17,97,100–103] and is involved in axonal regeneration and functional restoration in zebrafish after SCI [104,105]. Overexpression of BDNF has been shown to enhance both axonal regrowth and locomotor recovery in zebrafish [106,107], supporting the potential of targeting BDNF expression or signaling as a therapeutic approach for SCI in mammals. Studies on SCI showed that high BDNF levels are generally associated with better functional recovery, as it promotes cell survival and tissue regeneration both in mammals and in teleosts [108,109]. In the present study, BDNF expression revealed a significant variation among the experimental groups. Moreover, a previous study has shown that, after brain injury, the number of BDNF mRNA-expressing neurons markedly increases in the damaged area, with a greater number of BDNF-positive cells in the injured side compared to the contralateral uninjured side; although this expression gradually declines over time, it remains significantly elevated relative to controls, indicating a sustained neurotrophic response to injury [110]. In the current study, among the Ofe-treated groups, the Continuous SCI group displayed the highest BDNF expression. These findings indicate that Ofe vigorously enhances BDNF expression and that the magnitude of this effect is influenced by the timing of extract exposure. In contrast, the Curative SCI group, where treatment was initiated only after lesion induction, showed significantly lower BDNF expression compared to Continuous SCI, although still higher than the SCI group. This difference implies that delayed intervention may limit the capacity to fully activate neurotrophic signaling, emphasizing the importance of early treatment initiation in SCI recovery. These findings align with previous studies that emphasize the significance of BDNF in neuroprotection and recovery in SCI models [109], particularly in zebrafish, known for its regenerative capacity [111]. The Ofe-induced BDNF upregulation could be explained by the known capacity of flavonoids such as kaempferol [112] and quercetin [113] to activate the PI3K/Akt pathway, which in turn stimulates the mechanistic target of rapamycin (mTOR), a key regulator of protein synthesis including BDNF production [114]. This leads to increased local availability of BDNF. Additionally, PI3K/Akt activation inhibits apoptosis [115] and promotes cellular resilience in injured spinal cord tissues by suppressing pro-apoptotic factors [116]. These findings align with previous studies that emphasize the significance of BDNF in neuroprotection and recovery in SCI models [109].

3.8. Analysis of Sonic Hedgehog (shh, nestin, ngn1)-Related Gene Expression

Following SCI in zebrafish larvae, the expression of key genes involved in neurogenesis, including *Sonic Hedgehog* (*shh*), *nestin*, and *neurogenin1* (*ngn1*), was assessed. These genes are components of the Sonic Hedgehog (Shh) signaling pathway, which plays a pivotal role in activating neural progenitors and promoting neuronal regeneration after injury [117,118]. The secretion and activation of the Shh molecule are critical for regulating central nervous system polarity and neural patterning [119]. Moreover, this pathway governs fundamental developmental processes, including the growth and patterning of multicellular embryos [120,121]. In zebrafish, Shh signaling also interacts with other pathways, including fibroblast growth factor (FGF), to promote myelination and neuronal plasticity, emphasizing the relevance of these interactions for functional recovery in SCI models [122]. Secreted by the notochord into the neural tube, *Shh* is essential for the development of floor plate cells, motor neurons, and interneurons [123]. In vitro studies have shown that *Shh* enhances neurite outgrowth from dorsal root ganglion neurons and acts as a mitogen by promoting the proliferation of adult neural progenitor cells [124]. Moreover, in a murine SCI model, long-term release of *Shh* from implanted biodegradable microspheres improved functional recovery [125]. In the present study, RT-PCR analysis revealed a significant increase in the expression of *Shh* in all the treated groups compared to the SCI group, with the most pronounced increase reported in the Continuous SCI group. This upregulation could be attributed to the combined effects of preconditioning and sustained therapeutic intervention, as treatment was administered both before and after SCI. Pre-injury treatment likely enhanced tissue resilience by activating protective pathways, including Sonic Hedgehog-mediated neuronal survival [126], while post-injury treatment likely improved regenerative processes by sustaining *Shh*-driven effects, including tissue repair, progenitor cell recruitment, and angiogenesis [127]. *Nestin*, the second gene analyzed, also showed a post-injury upregulation, indicating the differentiation of mature cells into a progenitor-like state, an essential process for glial bridging and neuronal regeneration [128]. *Nestin* is also recognized as a marker for neural stem cells and precursor cells in mammals and zebrafish [129–131]. Its increase in treated groups, particularly in the Continuous SCI group, suggests that the administration of the polyphenol-rich extract both before and after SCI may enhance regenerative potential. Such an effect is likely attributed to the bioactive compounds identified in the extract, for which several studies have already reported the individual effects, demonstrating their ability to upregulate various processes involved in SCI repair [132–135]. Furthermore, the expression *Ngn1*, another neurogenic transcription factor regulating the differentiation of progenitor cells into neurons, was evaluated. Upregulation of *Ngn1* was observed in all treated groups, again with the highest expression in the Continuous SCI group, suggesting that Ofe may facilitate neuronal differentiation and contribute to the recovery of lost neural circuitry following SCI. Taken together, these results suggest that Ofe may enhance the activation of regenerative pathways, supporting neural repair and neurogenesis. The Continuous SCI group exhibited the most promising results, with upregulation of all three genes analyzed in the Sonic Hedgehog pathway supporting the hypothesis that combined pre- and post-injury administration maximizes therapeutic benefit.

Although Ofe treatment was associated with *Shh* pathway-related gene (*shh, nestin, ngn1*) upregulation in injured larvae, the present study does not establish a direct causal requirement for these pathways in mediating functional recovery. Future work therefore combining pathway-interference approaches (genetic loss-of-function and/or pharmacological inhibition of PI3K/Akt signaling) with the SCI paradigm, determining whether disrupting these signaling nodes abolishes Ofe-dependent benefits, would be of great interest.

4. Materials and Methods

4.1. Chemicals and Analytical Methods

4.1.1. Chemicals and Reagents

MS-grade methanol (MeOH) and water were supplied by Romil (Cambridge, UK). Ultrapure water (18 MΩ) was prepared by a Milli-Q purification system (Millipore, Burlington, MA, USA) were supplied by Sigma-Aldrich. Standard rutin (≥98% HPLC), quercetin (≥98% HPLC), and kaempferol (≥98% HPLC) were purchased from Sigma-Aldrich (Waltham, MA, USA).

4.1.2. Sample Collection

Prickly pear fruits were provided by the organic farm "Bruno" (Enna, Sicily, Italy). Samples were collected at the unripe stage of ripeness, during the practice of "scozzolatura", in June. All fruits were grown under equal agronomic and environmental conditions. After the collection, the samples were dried using a freeze-dryer (ALPHA 1-2 LSC BASIC, Martin Christ, Osterode am Harz, Germany) and stored at 4 °C for further testing.

4.1.3. Extraction and Sample Preparation

The hydroalcoholic extraction of unripe *Opuntia ficus-indica* fruits was conducted following the method described in a previous study [32]. The dried material was then ground into a fine powder. Next, 250 mg of the powder was weighed for each extraction, and 5 mL of an EtOH-H2O solution (50% v/v) was added. Sonication was performed at room temperature in an ultrasonic bath for three cycles, each lasting 10 min. The supernatants were collected by centrifugation at 6000 rpm for 5 min. The combined supernatants (15 mL) were transferred into a glass flask, and the organic solvent was removed using a Rotavapor. The remaining aqueous samples were frozen at −80 °C overnight and subsequently freeze-dried to obtain the final dry extract.

4.1.4. In Silico Prediction of Biological Activities

Potential biological activities were predicted using PASS Online (Prediction of Activity Spectra for Substances) [https://way2drug.com/PassOnline/] (accessed on 22 December 2025). Molecular structures were submitted in SMILES format. PASS Online provides the probability of each predicted activity being active (Pa) or inactive (Pi), ranging from 0 to 1. Predicted activities with Pa > Pi were considered reliable.

4.1.5. Spectrophotometric Assay for Antioxidant Activities (ABTS and DPPH Assays)

The radical scavenging activity of the extracts was assessed using the 1,1-diphenyl-2-picrylhydrazyl radical (DPPH•) and 2,2-azinobis-(3-ethylbenzothiazoline-6-sulfonate radical cation) (ABTS•+), following slightly modified protocols from Cannavacciuolo et al. [136]. Specifically, 50 µL of the extract (1 mg mL^{-1}) or standard solution (2.5–10 µg mL^{-1}) was mixed with 950 µL of a prepared DPPH• solution (0.14 mM). After a 30-min incubation in the dark at room temperature, the absorbance was measured at 515 nm using a spectrophotometer. For ABTS•+ scavenging activity, 50 µL of the extract was added to 950 µL of a diluted ABTS solution (14 mM), and the absorbance was recorded at 734 nm. All experiments were performed in triplicate. Absorbance values were calculated relative to a blank control (50% EtOH) and plotted against the concentration of the tested compound or the standard, 6-hydroxy-2,5,7,8-tetramethylchroman-2-carboxylic acid (Trolox). The antioxidant activity was expressed as Trolox equivalents (TE), representing the µmol of Trolox per gram of extract.

4.1.6. Characterization of *Opuntia ficus-indica* Extract Using High-Resolution Mass Spectrometry (QTOF–HRMS/MS)

UHPLC–QTOF–HRMS/MS analysis used an electrospray ionization (ESI) source integrated with a liquid chromatography and high-resolution mass spectrometry system. The setup included a Waters ACQUITY UPLC system coupled to a Waters Xevo G2-XS QTof mass spectrometer (Waters Corp., Milford, MA, USA), operating in both positive and negative ionization modes. Chromatographic separation was achieved on a Biphenyl column (100 mm × 2.1 mm, 2.6 µm; Phenomenex, Torrance, CA, USA) using a mobile phase of 0.1% (*v*/*v*) formic acid in water (A) and 0.1% (*v*/*v*) formic acid in acetonitrile (B) at a flow rate of 0.4 mL min^{-1}. The gradient elution consisted of 5% to 10% B for 2 min, followed by an increase to 80% B from 2.0 to 17.0 min, and then to 95% B for 1 min. The column was washed at 95% B for 5 min and equilibrated at 5% B for 3 min before the next injection. A 5 µL injection volume was used for each sample, prepared at a concentration of 0.5 mg mL^{-1}. The ESI source was operated with an electrospray capillary voltage of 2.5 kV, a source temperature of 150 °C, and a desolvation temperature of 500 °C. Mass spectra were recorded across a mass range of 50–1200 m/z using full-range acquisition. HRMS/MS data were obtained through data-dependent scanning, targeting the two most intense ions from the HRMS scan for collision-induced dissociation. Conditions included a minimum signal threshold of 250, an isolation width of 2.0, and a normalized collision energy of 30%. A resolving power of 30,000 was employed in both full-scan and MS/MS modes. Data processing and chemical identification were performed using ChemSpider database updated at the year 2025 and MS-FINDER software (version 3.6), with MS/MS spectra compared against the ChemSpider database and a custom library of phenolic compounds, supplemented by the literature references for confirmation.

4.1.7. Semiquantitative Analysis

Semiquantitative analysis was performed by preparing stock solutions (1 mg mL^{-1}) of the compounds used as external standards dissolved in a 50% methanol:water solution as solvent. The calibration curve was established by UHPLC-UV analysis with the wavelength set at 280 nm using a mixture of different standard solutions at 6 different concentrations (0.1, 0.5, 1, 5, 10, and 50 μg mL^{-1}) and 5 μL of each concentration was injected in technical triplicate. The calibration curves were obtained by linear regression using Excel 2016 software, reporting the area of the external standards against the known concentration of each standard. The calibration curves obtained showed good linearity with correlation coefficients (R2) between 0.9975 and 0.9998. Quantitative data are expressed as ug g^{-1} of dry extract (EXT). MassLynx software (version 4.2) was used for instrument control, data acquisition, and processing.

4.2. Zebrafish Husbandry

Zebrafish (*Danio rerio*) used in this study were maintained in two independent facilities for distinct experimental phases, namely the zebrafish embryo toxicity test (ZFET) and the in vivo spinal cord injury (SCI) experiments. In both facilities, animals were housed under standardized conditions in accordance with international guidelines for zebrafish care and use.

4.2.1. Zebrafish Maintenance for ZFET

For the zebrafish embryo toxicity test, zebrafish (*Danio rerio*) were bred at the European Zebrafish Resource Center (EZRC) at the Karlsruhe Institute of Technology (Karlsruhe, Germany) in a flow-through system (Aqua Schwarz and Müller + Pfleger). Adult zebrafish were housed in 15 L tanks with a maximum of 24 fish per tank, maintained on a 14-h light/10-h dark cycle. The water temperature was kept at 28.5 °C with a conductivity of 200 μS, and the water was continuously refreshed. The fish were fed three times daily with dry food and Artemia salina larvae. The afternoon before spawning, groups of males and females (1:1 ratio) were placed in 1 L breeding tanks (Tecniplast S.p.A., Buguggiate, Italy). After spawning, fertilized eggs were collected using a sieve, and then non-fertilized eggs or damaged embryos were discarded.

4.2.2. Zebrafish Maintenance for SCI Experiments

Zebrafish AB (*Danio rerio*) were maintained at the Institute for Comparative, Experimental, Forensic, and Aquatic Pathology "Slavko Bambir", Department of Chemical, Biological, Pharmaceutical, and Environmental Sciences of the University of Messina, Italy, in a self-contained system (ZebTec, Tecniplast, Italy) under controlled water conditions, with a 14 h light/10 h dark cycle, a temperature of 27–28 °C, a pH of 7.5, and 600 μS/cm conductivity. Fish were fed twice daily with Gemma micro 300 (Skretting, Varese, Italy) and Artemia salina, amounting to 3% of their body weight.

4.3. Zebrafish Embryonic Toxicity Test

The acute toxicity of *Opuntia ficus-indica* extract (Ofe) on zebrafish embryos was assessed according to the "Fish Embryo Acute Toxicity (ZFET) Test," outlined in the OECD Guidelines for the Testing of Chemicals—Test No. 236 [137], using n = 216 wild-type AB line zebrafish embryos, randomly selected based on morphological normality and appropriate shape, delivered by EZRC, at the Institute of Biological and Chemical Systems-Biological Information Processing (IBCS-BIP), Karlsruhe Institute of Technology, Karlsruhe, Germany. The hydroalcoholic extract was dissolved in E3 medium to achieve final concentrations of 25, 50, 100, 200, 400, 800, and 1600 μg mL^{-1}. Embryos were individually placed in 24-well plates, with 2 mL of the respective solution per well. Thus, this assay has included nine groups. The number of embryos per group and the distribution of experimental and control wells were defined in strict accordance with OECD Test Guideline No. 236 [137]. For each Ofe experimental group, *n* = 20 embryos were used, while the remaining 4 wells were dedicated for internal negative control (E3 medium). Both solutions were freshly prepared and renewed every 24 h. Additionally, a negative control (E3 medium; *n* = 24) and a positive control plate (4% 3,4-dichloroaniline; *n* = 24) were included. The embryos were incubated at 28.5 °C, alternating plate position, for 96 h post-fertilization (hpf). To minimize potential stress, embryos were maintained under optimal environmental conditions and handled with minimal manipulation. Daily observations were conducted under an SMZ 645 stereomicroscope (SMZ 645 Nikon, Tokyo, Japan) all along the experiment. Lethality was assessed through four endpoints: (i) egg coagulation, (ii) absence of somite formation, (iii) failure of tail-bud detachment from the yolk sac, and (iv) lack of heartbeat. No unexpected adverse events occurred during the study. At the end of the exposure period, the 50% lethal concentration (LC50) was calculated. Morphological abnormalities were also documented. By the end of the experiment, embryos were euthanized by hypothermia procedure.

Group allocation was performed by one operator prior to the start of the experiment. During the exposure phase, the operator responsible for treatment administration and daily maintenance was aware of group assignment to ensure correct handling and renewal of solutions. However, during outcome assessment, experimental groups were identified by coded labels. Data collection and subsequent analysis were carried out by a second researcher who remained blinded to treatment group identities, thereby minimizing bias. To minimize potential confounding factors, all experimental groups were maintained under identical environmental conditions and assessed at the same developmental stage and time points. The analyses were performed using the same experimental setup across groups. Moreover, all experimental groups were processed using a predefined order of plates during daily medium changes and subsequent experimental procedures.

ZFET Test Data Analysis

No animals or data points were excluded from the analysis. The concentration–response curves derived from the ZFET data were analyzed using the PROAST web tool for benchmark dose (BMD) analysis, based on PROAST software version 70.1, developed by the Dutch Institute for Public Health and the Environment (RIVM, The Netherlands) [138]. The benchmark concentration (BMC) at a predefined benchmark response (BMR) was calculated by fitting a dose–response curve. The LC50 value was obtained from the concentration–response curves generated in the ZFET test. In this case, the BMR was set to 50%, representing the concentration that caused either 50% cumulative mortality or lethality (LC50). GraphPad Prism 8.0 was used to generate figures of the concentration–response curves for the test compounds in the ZFET test.

4.4. Spinal Cord Transection Technique

To perform spinal cord transection (SCI), 3 dpf zebrafish larvae were prior anesthetized in E3 medium containing 0.01% Tricaine methanesulfonate (MS-222, Sigma-Aldrich, St. Louis, MO, USA), using 1 mL of 0.4% MS-222 in 40 mL of medium (larvae were sufficiently anesthetized when no response to touch was observed), then transferred to an agar plate and positioned by direct visualization under a stereomicroscope (Leica M205C equipped with a Leica IC80 HD digital camera, Leica, Milan, Italy). Excess E3 medium was carefully removed with an aspiration pipette, allowing the larvae to settle laterally on the plate. The larva was then approached from the dorsal side with a 30 G needle at the level of the 15th myotome, positioning the needle with its bevel facing sideways, taking care to avoid damage to the notochord, as previously described [89,139]. After the incision, each lesioned larva was flushed gently off the surgical plate with a transfer pipette and transferred to an individual well of a 24-well plate filled with fresh E3 solution to recover for 1 h. Then, the larvae were placed in wells filled with the respective medium and kept in the incubator at 28.5 °C. On the same day of the surgery, dead or notochord-damaged larvae were removed, and the lesioned larvae were monitored daily. All procedures were performed under a stereomicroscope (Leica M205C equipped with a Leica IC80 HD digital camera, Leica, Milan, Italy).

4.4.1. Experimental Design and Treatment with *Opuntia ficus-indica* Extract

The experimental design included six groups (n = 20 larvae per group, with three independent replicates) to distinguish the effects of SCI from those of the treatment. The Ctrl (Control) group, serving as the uninjured baseline, was maintained in E3 medium for the entire duration of the experiment without SCI or exposure to the *Opuntia ficus-indica extract* (Ofe). The SCI group acted as the injury control; larvae were also kept in E3 medium but subjected to SCI at 72 h post-fertilization (hpf) without receiving Ofe. In addition, treatment groups were organized to assess the biological activity of the Ofe under distinct exposure timepoints. The Continuous SCI group received Ofe freshly prepared in E3 medium at a final concentration of 50 μg/mL, from 0 to 120 hpf, comprising both pre and post SCI. The Continuous group followed the same extract administration without SCI, serving to isolate the effects of Ofe in non-injured larvae. The Curative SCI group was maintained in E3 medium until SCI induction at 72 hpf and subsequently treated with Ofe until 120 hpf. The Curative group was subjected to an identical post-72 hpf treatment in the absence of SCI, serving as a control for late-onset extract exposure. The organization of the experimental groups and the corresponding treatment timeline is shown in Figure 10. Group allocation was performed by one operator prior to the start of the experiment. During the exposure phase, the operator conducting the treatments and daily maintenance was aware of group assignment to ensure correct handling of solutions. However, outcome assessment and data analysis were carried out by a second researcher blinded to the treatment groups to minimize bias. To minimize potential confounding factors, all experimental groups were maintained under identical environmental conditions and assessed at the same developmental stage and time points. The analyses were performed using the same experimental setup across groups. Moreover, all experimental groups were processed using a predefined order of plates during daily medium changes and subsequent experimental procedures. Sample size was determined based on previous zebrafish studies and practical considerations.

4.4.2. DanioVisionTM Observation System for Behavior Assessment

Locomotor activity recovery in larvae was assessed using the Danio Vision system as described in [17]. By the end of the experiment, at 120 hpf, larvae were placed in individual wells of a 24-well transparent spot plate with 1 mL of E3 medium. After a 10-min acclimation in the dark, the behavioral activity of zebrafish larvae was recorded for 120 min using the DanioVision^{TM} observation system (Noldus, Wageningen, The Netherlands, Model: 17.0.1630). The behavioral assay was conducted in a temperature-controlled room at 26 ± 1 °C, and the light intensity was adjusted to 2412 lux. Each zebrafish larva's accumulated behavioral data activity was analyzed for two endpoints. The total distance traveled and the velocity were calculated using Ethovision$^{®}$XT (Noldus, VA, USA). Following behavioral assessment with the DanioVisionTM system, larvae were observed and photographed using a Leica stereomicroscope to document the lesion site and monitor morphological indicators of recovery. The optical transparency of zebrafish larvae enables high-resolution in vivo imaging of spinal cord regeneration, providing a reliable qualitative evaluation of structural recovery over time.

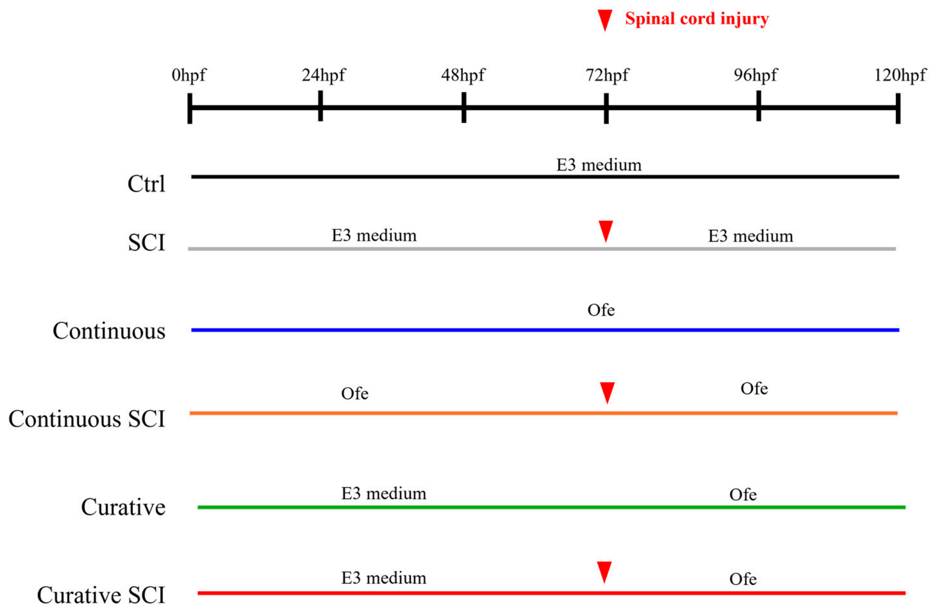

Figure 10. Experimental design and treatment schedule. Ctrl (Control, uninjured) group, SCI group (spinal cord injury, without *Opuntia ficus*-indica extract-Ofe-treatment), Continuous SCI group (SCI treated with Ofe from 0 to 120 hpf), Continuous group (treatment with Ofe from 0 to 120 hpf without SCI), Curative SCI group (SCI treated with Ofe after 72 hpf), and Curative group (treatment with Ofe after 72 hpf without SCI).

4.4.3. Assessment of Wound Healing

Lesion area was quantified at T0 and 2 dpi for each of the ten larvae. Images were acquired using a stereomicroscope (Leica M205C equipped with a Leica IC80 HD digital camera, Leica, Milan, Italy) under identical acquisition settings. Lesion area was measured using ImageJ (ImageJ/Fiji, version 1.54 h, National Institutes of Health, Bethesda, MD USA). Measurements were expressed in μm^2.

4.4.4. Molecular Analyses

Gene expression analyses complied with the minimum information for publication of quantitative real-time PCR experiments, MIQE guidelines [140–142]. Total RNA was extracted from pools of 15 randomly selected larvae per experimental group using the QIAzol® Lysis Reagent (QIAGEN® Inc., Valencia, CA, USA, Cat. # 79306). The RNA was quantified using a NanoDrop® ND-1000 spectrophotometer (Thermo Fisher Scientific, Wilmington, NC, USA), and the quality was verified by running 500 ng of RNA on a 1% agarose gel. Two micrograms of total RNA were reverse transcribed into cDNA using the QuantiTect® Reverse Transcription Kit (QIAGEN Gmbh, Hilden, Germany, Cat. 205313). The analysis was carried out in triplicate, using the iTaq™ Universal SYBR® Green Supermix (Bio-Rad Laboratories Inc., Hercules, CA, USA, Cat. #1725124). The primers were designed using NCBI Primer-BLAST + 2.17.0 (https://www.ncbi.nlm.nih.gov/tools/primer-blast/, accessed on: 3 July 2025) [143] to bind the sequences of the here-studied genes. See Table 5 for the primer sequence details. Samples were amplified with the primers for each target gene, and for all these genes, one no-template control (NTC) sample was run. Raw data (CT) were analyzed with "Biogazelle qbase plus" software version 2.3, and the fold changes (versus the starvation value) were expressed as CNRQ (calibrated normalized relative quantity) of the means with standard error (S.E.). Beta-actin and EF-1 alpha were used as housekeeping genes. The starvation values are reported as $2^{-\Delta\Delta CT}$.

Table 5. Primers for RT-PCR.

Gene	Primer Orientation	Nucleotide Sequence
neurogenin 1	forward	GAG GGT TAA GAG CAA GAC AGA C
	reverse	CTG GGA GAT GCT TGA GGT TT
sonic hedgehog a	forward	TGT CTC TTC TCA CTC TGT CCT T
	reverse	CAG CTT CTT CGG ATG TCT TCT T
nestin	forward	CAA CAT CTT CAG GCC CAA GTA A
	reverse	CCT GCA GCA GAT GTT GTC TAT C
BDNF	forward	GCA CGG CAG AAG TTC TCA TA
	reverse	CCT ATG CTG TCC TGG AGA TAG A
IL-8	forward	CTC TGC TCC ATG GGT TAA GAA G
	reverse	AAC TTG ACT TCA CAG GTG ATC C
il1β	forward	AGT GAA CGT GGT GGA TTC AG
	reverse	TGC GCA CAG AGA CTT CTT ATA C
TNF-α	forward	CTT CCT CAG ACC ACG GAA A
	reverse	CGA TTG TCC TGA AGG GTC A
Beta-actin	forward	AAAGCTGTGACCCACCTCAC
	reverse	CAGCTGGTCGTATCCGTTTG
EF-1 alpha	forward	TGTCCTCAAGCCTGGTATGG
	reverse	TGGGTCGTTCTTGCTGTCTC

4.5. Statistical Analysis

Statistical analyses were conducted, and graphs were created using IBM SPSS Statistics for Windows version 22 (IBM Corp., Armonk, NY, USA) and GraphPad Prism version 8.0.1 for Windows (GraphPad Software, San Diego, CA, USA) as described previously. After confirming data normality and homogeneity of variance, differences between the groups were analyzed using one-way ANOVA for normally distributed data with equality of variance, the Welch's t-test for normally distributed data with unequal variances, or the Mann–Whitney U test for non-normal distributions [144]. Values are expressed as mean ± SE except for total polyphenol and flavonoid content, DPPH and ABTS radical scavenging, and glucosidase enzyme inhibition, which were performed in triplicate, and the results are expressed as mean ± SD, and the significance threshold was established as the p-value ($p < 0.05$).

5. Conclusions

This work provides an integrated evaluation of the unripe *Opuntia ficus-indica* hydroalcoholic extract (Ofe). By combining chemical characterization, embryotoxicity assessment, and in vivo functional evaluation, this study aims to expand the current knowledge on *Opuntia ficus-indica*, a plant that is gaining increasing attention for its biological properties, and establishes a methodological framework for investigating plant-derived extracts in a zebrafish model of spinal cord injury, thereby supporting its potential use in new experimental contexts. The extract was shown to influence locomotor performance and molecular responses associated with the post-injury microenvironment, indicating its capacity to modulate injury-related processes rather than acting through a single pathway. Differences observed between treatment regimens further emphasize the relevance of exposure timing and duration in shaping biological outcomes.

Overall, the present findings support unripe *O. ficus-indica* extract as a source of bioactive compounds for experimental studies aimed at exploring the modulation of spinal cord injury-associated responses. Future investigations will be required to directly compare unripe and ripe fruit extracts in parallel chemical and in vivo assays and test the causal contribution of neurotrophic/neurogenic candidate pathways using genetic or pharmacological interference. Moreover, isolating the contribution of individual Ofe components, perhaps using mammalian models of spinal cord injury, may clarify their translational significance and define their potential clinical implications.

Supplementary Materials: The following supporting information can be downloaded at: https://www.mdpi.com/article/10.3390/ijms27041687/s1.

Author Contributions: Conceptualization, G.M. and L.C.; methodology, L.C.; L.P.; K.M.; M.A.; S.P.; software, L.P.; K.M.; S.P.; M.L. (Massimo Labra), M.S.; validation, M.L. (Maria Levanti); R.L.; S.R.; A.G.; M.L. (Massimo Labra); N.C.; M.G.; M.R.C.; F.A. and G.M.; formal analysis, L.P.; M.A.; K.M.; S.P.; investigation, L.P.; K.M.; M.A.; M.S.; S.P.; resources, M.L. (Massimo Labra); L.C.; A.G.; G.M.; data curation, L.P.; K.M.; M.A.; S.P.; M.S.; writing—original draft preparation, L.P.; K.M.; M.A.; M.S. S.P.; writing—review and editing, M.L. (Maria Levanti); R.L.; S.R.; A.G.; M.L. (Massimo Labra); N.C.; M.G.; M.R.C.; F.A., and G.M.; visualization, M.L. (Maria Levanti); R.L.; S.R.; A.G.; M.L. (Massimo Labra); N.C.; M.G.; M.R.C.; F.A. and G.M.; supervision, A.G.; G.M.; L.C.; project administration, A.G.; G.M.; L.C.; funding acquisition, G.M.; L.C.; M.L. (Massimo Labra). All authors have read and agreed to the published version of the manuscript.

Funding: Project funded under the National Recovery and Resilience Plan (NRRP), Mission 4. Component 2 Investment 1.3—Call for tender No. 3138, 16 December 2021, rectified by Decree n. 341 of 15 March 2022 of the Italian Ministry of University and Research funded by the European Union—NextGenerationEU; Project code PE0000003 ON FOODS—CUP:H43C22000820001—Spoke 6, Project title "ON Foods—Research and innovation network on food and nutrition Sustainability, Safety and Security—Working ON Foods". Programma Operativo Nazionale Ricerca e Innovazione 2024-2020 (CCI 2014IT 6M2OP005) Fondo Sociale Europeo, Azione I. 1 "Dottorati Innovativi con caratterizzazione Industriale".

Institutional Review Board Statement: Experimental procedures conducted in Germany were performed at the Karlsruhe Institute of Technology (KIT), a facility authorized by the Regierungspräsidium Karlsruhe in accordance with §11 of the German Animal Welfare Act (TierSchG) (approval reference:35-9185.64/BH KIT, approval date: 15 November 2023).). Zebrafish (Danio rerio) were housed and maintained at the KIT in compliance with the guidelines of the European Society for Fish Models in Biology and Medicine (EuFishBioMed). All experiments were conducted on embryos up to 120 h post-fertilization (hpf), which are not classified as protected animals under Directive 2010/63/EU of the European Parliament and of the Council. The study adheres to the ARRIVE (Animal Research: Reporting of In Vivo Experiments) guidelines to ensure transparent and reproducible reporting. Experiments on zebrafish larvae conducted in Italy were performed without ethical approval since, according to Directive 2010/63/EU, transposed into Italian law by D.lgs. 26/2014 on the protection of animals used for scientific research, zebrafish larvae up to five days (120 hpf) are not considered protected zebrafish forms and thus do not need ethical approval.

Informed Consent Statement: Not applicable.

Data Availability Statement: All data presented in this study are available from the corresponding author upon responsible request.

Acknowledgments: We are grateful to the National Biodiversity Future Center (NBFC), Palermo, Italy (funded by the European Union's Next Generation EU; Project code CN00000033; CUP:

H43C22000530001). The authors sincerely thank Azienda Bruno for providing the *Opuntia ficus-indica* samples used in this study.

Conflicts of Interest: We confirm that Dr. Nicola Cicero is affiliated with the Science4Life Spin-off Company, which is a research spin-off within the Department of Veterinary Sciences of the University of Messina. A minimal part of the extraction procedures was conducted at this institution. The spin-off had no role in the study design, data analysis, interpretation of results, or manuscript preparation, and no financial or non-financial conflicts of interest were present.

References

1. Hellenbrand, D.J.; Quinn, C.M.; Piper, Z.J.; Morehouse, C.N.; Fixel, J.A.; Hanna, A.S. Inflammation after Spinal Cord Injury: A Review of the Critical Timeline of Signaling Cues and Cellular Infiltration. *J. Neuroinflamm.* **2021**, *18*, 284. [CrossRef] [PubMed]
2. Beattie, M.S.; Li, Q.; Bresnahan, J.C. Cell Death and Plasticity after Experimental Spinal Cord Injury. *Prog. Brain Res.* **2000**, *128*, 9–21. [PubMed]
3. Schwab, M.E.; Bartholdi, D. Degeneration and Regeneration of Axons in the Lesioned Spinal Cord. *Physiol. Rev.* **1996**, *76*, 319–370. [CrossRef]
4. Ahuja, C.S.; Wilson, J.R.; Nori, S.; Kotter, M.; Druschel, C.; Curt, A.; Fehlings, M.G. Traumatic Spinal Cord Injury. *Nat. Rev. Dis. Primers* **2017**, *3*, 17018. [CrossRef]
5. Alizadeh, A.; Dyck, S.M.; Karimi-Abdolrezaee, S. Traumatic Spinal Cord Injury: An Overview of Pathophysiology, Models and Acute Injury Mechanisms. *Front. Neurol.* **2019**, *10*, 282. [CrossRef]
6. Hall, E.D. Antioxidant Therapies for Acute Spinal Cord Injury. *Neurotherapeutics* **2011**, *8*, 152–167. [CrossRef]
7. Fawcett, J.W.; Asher, R.A. The Glial Scar and Central Nervous System Repair. *Brain Res. Bull.* **1999**, *49*, 377–391. [CrossRef]
8. Alper, S.R.; Dorsky, R.I. Unique Advantages of Zebrafish Larvae as a Model for Spinal Cord Regeneration. *Front. Mol. Neurosci.* **2022**, *15*, 983336. [CrossRef]
9. Mhalhel, K.; Sicari, M.; Pansera, L.; Chen, J.; Levanti, M.; Diotel, N.; Rastegar, S.; Germanà, A.; Montalbano, G. Zebrafish: A Model Deciphering the Impact of Flavonoids on Neurodegenerative Disorders. *Cells* **2023**, *12*, 252. [CrossRef]
10. Pansera, L.; Mhalhel, K.; Cavallaro, M.; Aragona, M.; Laurà, R.; Levanti, M.; Guerrera, M.C.; Abbate, F.; Germanà, A.; Montalbano, G. Zebrafish as an Integrative Model for Central Nervous System Research: Current Advances and Translational Perspectives. *Life* **2025**, *15*, 1751. [CrossRef] [PubMed]
11. Aragona, M.; Porcino, C.; Briglia, M.; Mhalhel, K.; Abbate, F.; Levanti, M.; Montalbano, G.; Laurà, R.; Lauriano, E.R.; Germanà, A.; et al. Vimentin Localization in the Zebrafish Oral Cavity: A Potential Role in Taste Buds Regeneration. *Int. J. Mol. Sci.* **2023**, *24*, 15619. [CrossRef]
12. Montalbano, G.; Mhalhel, K.; Briglia, M.; Levanti, M.; Abbate, F.; Guerrera, M.C.; D'Alessandro, E.; Laurà, R.; Germanà, A. Zebrafish and Flavonoids: Adjuvants against Obesity. *Molecules* **2021**, *26*, 3014. [CrossRef] [PubMed]
13. Bhatt, D.H.; Otto, S.J.; Depoister, B.; Fetcho, J.R. Cyclic AMP-Induced Repair of Zebrafish Spinal Circuits. *Science* **2004**, *305*, 254–258. [CrossRef] [PubMed]
14. Briona, L.K.; Poulain, F.E.; Mosimann, C.; Dorsky, R.I. Wnt/ß-Catenin Signaling Is Required for Radial Glial Neurogenesis Following Spinal Cord Injury. *Dev. Biol.* **2015**, *403*, 15–21. [CrossRef]
15. Ohnmacht, J.; Yang, Y.; Maurer, G.W.; Barreiro-Iglesias, A.; Tsarouchas, T.M.; Wehner, D.; Sieger, D.; Becker, C.G.; Becker, T. Spinal Motor Neurons Are Regenerated after Mechanical Lesion and Genetic Ablation in Larval Zebrafish. *Development* **2016**, *143*, 1464–1474. [CrossRef] [PubMed]
16. Kuil, L.E.; Chauhan, R.K.; Cheng, W.W.; Hofstra, R.M.; Alves, M.M. Zebrafish: A Model Organism for Studying Enteric Nervous System Development and Disease. *Front. Cell Dev. Biol.* **2021**, *8*, 629073. [CrossRef]
17. Mhalhel, K.; Kadmi, Y.; Ben Chira, A.; Levanti, M.; Pansera, L.; Cometa, M.; Sicari, M.; Germanà, A.; Aragona, M.; Montalbano, G. Urtica Dioica Extract Abrogates Chlorpyrifos-Induced Toxicity in Zebrafish Larvae. *Int. J. Mol. Sci.* **2024**, *25*, 6631. [CrossRef]
18. Keatinge, M.; Tsarouchas, T.M.; Munir, T.; Porter, N.J.; Larraz, J.; Gianni, D.; Tsai, H.-H.; Becker, C.G.; Lyons, D.A.; Becker, T. CRISPR gRNA Phenotypic Screening in Zebrafish Reveals Pro-Regenerative Genes in Spinal Cord Injury. *PLoS Genet.* **2021**, *17*, e1009515. [CrossRef]
19. Aragona, M.; Lauriano, E.R.; Pergolizzi, S.; Faggio, C. *Opuntia ficus-indica* (L.) Miller as a Source of Bioactivity Compounds for Health and Nutrition. *Nat. Prod. Res.* **2018**, *32*, 2037–2049. [CrossRef]
20. Cueto-Escobedo, J.; German-Ponciano, L.J.; Guillén-Ruiz, G.; Soria-Fregozo, C.; Herrera-Huerta, E.V. Zebrafish as a Useful Tool in the Research of Natural Products with Potential Anxiolytic Effects. *Front. Behav. Neurosci.* **2022**, *15*, 795285. [CrossRef]
21. Lin, F.-J.; Li, H.; Wu, D.-T.; Zhuang, Q.-G.; Li, H.-B.; Geng, F.; Gan, R.-Y. Recent Development in Zebrafish Model for Bioactivity and Safety Evaluation of Natural Products. *Crit. Rev. Food Sci. Nutr.* **2022**, *62*, 8646–8674. [CrossRef]

22. Al-Khayri, J.M.; Sahana, G.R.; Nagella, P.; Joseph, B.V.; Alessa, F.M.; Al-Mssallem, M.Q. Flavonoids as Potential Anti-Inflammatory Molecules: A Review. *Molecules* **2022**, *27*, 2901. [CrossRef]
23. Rao, M.J.; Duan, M.; Zhou, C.; Jiao, J.; Cheng, P.; Yang, L.; Wei, W.; Shen, Q.; Ji, P.; Yang, Y. Antioxidant Defense System in Plants: Reactive Oxygen Species Production, Signaling, and Scavenging during Abiotic Stress-Induced Oxidative Damage. *Horticulturae* **2025**, *11*, 477. [CrossRef]
24. Shamsudin, N.F.; Ahmed, Q.U.; Mahmood, S.; Shah, S.A.A.; Sarian, M.N.; Khattak, M.M.A.K.; Khatib, A.; Sabere, A.S.M.; Yusoff, Y.M.; Latip, J. Flavonoids as Antidiabetic and Anti-Inflammatory Agents: A Review on Structural Activity Relationship-Based Studies and Meta-Analysis. *Int. J. Mol. Sci.* **2022**, *23*, 12605. [CrossRef] [PubMed]
25. Li, S.; Gao, S.; Hu, Y.; Feng, J.; Sheng, W. Research Progress of Flavonoids in Spinal Cord Injury: Therapeutic Mechanisms and Drug Delivery Strategies. *Phytother. Res.* **2025**, *39*, 2555–2570. [CrossRef] [PubMed]
26. Zhang, Q.; Liu, M.; Nong, H.; Zhang, Y.; Bai, Y.; Liu, P.; Zong, S.; Zeng, G. Total Flavonoids of Hawthorn Leaves Protect Spinal Motor Neurons via Promotion of Autophagy after Spinal Cord Injury. *Front. Pharmacol.* **2022**, *13*, 925568. [CrossRef] [PubMed]
27. El-Mostafa, K.; El Kharrassi, Y.; Badreddine, A.; Andreoletti, P.; Vamecq, J.; El Kebbaj, M.S.; Latruffe, N.; Lizard, G.; Nasser, B.; Cherkaoui-Malki, M. Nopal Cactus (*Opuntia ficus-indica*) as a Source of Bioactive Compounds for Nutrition, Health and Disease. *Molecules* **2014**, *19*, 14879–14901. [CrossRef]
28. Iftikhar, K.; Siddique, F.; Ameer, K.; Arshad, M.; Kharal, S.; Mohamed Ahmed, I.A.; Yasmin, Z.; Aziz, N. Phytochemical Profiling, Antimicrobial, and Antioxidant Activities of Hydroethanolic Extracts of Prickly Pear (*Opuntia ficus indica*) Fruit and Pulp. *Food Sci. Nutr.* **2023**, *11*, 1916–1930. [CrossRef]
29. Liao, H.; Zhao, Y.; Liang, Y.; Zou, K. Flavonoids Derived from *Opuntia ficus-indica* Fruit Alleviate Renal Injury in Diabetic Nephropathy Mice by Altering Gut Microbiota and Promoting the Production of SCFAs. *Nutrients* **2025**, *17*, 1800. [CrossRef]
30. Shoukat, R.; Cappai, M.; Pia, G.; Pilia, L. An Updated Review: *Opuntia ficus indica* (OFI) Chemistry and Its Diverse Applications. *Appl. Sci.* **2023**, *13*, 7724. [CrossRef]
31. Huang, Z.; Wang, J.; Li, C.; Zheng, W.; He, J.; Wu, Z.; Tang, J. Application of Natural Antioxidants from Traditional Chinese Medicine in the Treatment of Spinal Cord Injury. *Front. Pharmacol.* **2022**, *13*, 976757. [CrossRef]
32. Wu, Z.; Wu, W.; Ding, X.; Feng, Q.; Zhang, B.; Wang, H.; Cui, X.; Yao, M. Neuroprotective Effect and Possible Mechanisms of the Extract of Ginkgo Biloba for Spinal Cord Injury in Experimental Animal: A Meta-Analysis and Systematic Review. *Nutr. Neurosci.* **2025**, *28*, 840–853. [CrossRef] [PubMed]
33. Maccioni, O.; Demuro, I.; Musmeci, S.; Procacci, S.; Mulas, M.; Bacchetta, L. Morphological, Physical, and Chemical Characterization of Cactus Pear (*Opuntia ficus-indica* [L.] Mill.) Fruits from Progressive Out-of-Season Harvests. *Appl. Fruit Sci.* **2025**, *67*, 282. [CrossRef]
34. Mata, A.; Ferreira, J.P.; Semedo, C.; Serra, T.; Duarte, C.M.M.; Bronze, M.R. Contribution to the Characterization of *Opuntia* Spp. Juices by LC–DAD–ESI-MS/MS. *Food Chem.* **2016**, *210*, 558–565. [CrossRef]
35. Kolniak-Ostek, J.; Kita, A.; Miedzianka, J.; Andreu-Coll, L.; Legua, P.; Hernandez, F. Characterization of Bioactive Compounds of *Opuntia ficus-indica* (L.) Mill. Seeds from Spanish Cultivars. *Molecules* **2020**, *25*, 5734. [CrossRef]
36. Jakabfi-Csepregi, R.; Alberti, Á.; Felegyi-Tóth, C.A.; Kőszegi, T.; Czigle, S.; Papp, N. A Comprehensive Study on *Lathyrus tuberosus* L.: Insights into Phytochemical Composition, Antimicrobial Activity, Antioxidant Capacity, Cytotoxic, and Cell Migration Effects. *Plants* **2024**, *13*, 232. [CrossRef]
37. Yeddes, N.; Chérif, J.K.; Trabelsi Ayadi, M. Comparative Study of Antioxidant Power, Polyphenols, Flavonoids and Betacyanins of Peel and Pulp of Three Tunisian Opuntia Forms. *Pak. J. Biol. Sci.* **2014**, *17*, 650–658. [CrossRef]
38. Engels, C.; Gräter, D.; Esquivel, P.; Jiménez, V.M.; Gänzle, M.G.; Schieber, A. Characterization of Phenolic Compounds in Jocote (*Spondias purpurea* L.) Peels by Ultra High-Performance Liquid Chromatography/Electrospray Ionization Mass Spectrometry. *Food Res. Int.* **2012**, *46*, 557–562. [CrossRef]
39. Ding, S.; Dudley, E.; Plummer, S.; Tang, J.; Newton, R.P.; Brenton, A.G. Fingerprint Profile of Ginkgo Biloba Nutritional Supplements by LC/ESI-MS/MS. *Phytochemistry* **2008**, *69*, 1555–1564. [CrossRef]
40. Ghareeb, M.; Saad, A.; Ahmed, W.; Refahy, L.; Nasr, S. HPLC-DAD-ESI-MS/MS Characterization of Bioactive Secondary Metabolites from Strelitzia Nicolai Leaf Extracts and Their Antioxidant and Anticancer Activities in Vitro. *Pharmacogn. Res.* **2018**, *10*, 368–378. [CrossRef]
41. Tesoro, C.; Lelario, F.; Piscitelli, F.; Di Capua, A.; Della Sala, P.; Montoro, P.; Bianco, G.; Acquavia, M.A.; Dell'Agli, M.; Piazza, S. *Vicia faba* L. Pod Valves: A By-Product with High Potential as an Adjuvant in the Treatment of Parkinson's Disease. *Molecules* **2024**, *29*, 3943. [CrossRef]
42. Burò, I.; Consoli, V.; Castellano, A.; Vanella, L.; Sorrenti, V. Beneficial Effects of Standardized Extracts from Wastes of Red Oranges and Olive Leaves. *Antioxidants* **2022**, *11*, 1496. [CrossRef]
43. Maina, S.; Kachrimanidou, V.; Koutinas, A. A Roadmap towards a Circular and Sustainable Bioeconomy through Waste Valorization. *Curr. Opin. Green Sustain. Chem.* **2017**, *8*, 18–23. [CrossRef]

44. Kim, J.-H.; Park, S.-M.; Ha, H.-J.; Moon, C.-J.; Shin, T.-K.; Kim, J.-M.; Lee, N.-H.; Kim, H.-C.; Jang, K.-J.; Wie, M.-B. *Opuntia ficus-indica* Attenuates Neuronal Injury in in Vitro and in Vivo Models of Cerebral Ischemia. *J. Ethnopharmacol.* **2006**, *104*, 257–262. [CrossRef]
45. Benayad, Z.; Martinez-Villaluenga, C.; Frias, J.; Gomez-Cordoves, C.; Es-Safi, N.E. Phenolic Composition, Antioxidant and Anti-Inflammatory Activities of Extracts from Moroccan *Opuntia ficus-indica* Flowers Obtained by Different Extraction Methods. *Ind. Crops Prod.* **2014**, *62*, 412–420. [CrossRef]
46. Matias, A.; Nunes, S.L.; Poejo, J.; Mecha, E.; Serra, A.T.; Madeira, P.J.A.; Bronze, M.R.; Duarte, C.M.M. Antioxidant and Anti-Inflammatory Activity of a Flavonoid-Rich Concentrate Recovered from *Opuntia ficus-indica* Juice. *Food Funct.* **2014**, *5*, 3269–3280. [CrossRef]
47. Cota-Sánchez, J.H. Chapter 28—Nutritional Composition of the Prickly Pear (*Opuntia ficus-indica*) Fruit. In *Nutritional Composition of Fruit Cultivars*; Simmonds, M.S.J., Preedy, V.R., Eds.; Academic Press: San Diego, CA, USA, 2016; pp. 691–712.
48. Guevara-Figueroa, T.; Jiménez-Islas, H.; Reyes-Escogido, M.L.; Mortensen, A.G.; Laursen, B.B.; Lin, L.-W.; De León-Rodríguez, A.; Fomsgaard, I.S.; Barba de la Rosa, A.P. Proximate Composition, Phenolic Acids, and Flavonoids Characterization of Commercial and Wild Nopal (*Opuntia* spp.). *J. Food Compos. Anal.* **2010**, *23*, 525–532. [CrossRef]
49. Gómez-Maqueo, A.; García-Cayuela, T.; Welti-Chanes, J.; Cano, M.P. Enhancement of Anti-Inflammatory and Antioxidant Activities of Prickly Pear Fruits by High Hydrostatic Pressure: A Chemical and Microstructural Approach. *Innov. Food Sci. Emerg. Technol.* **2019**, *54*, 132–142. [CrossRef]
50. Hernández, F.; Andreu-Coll, L.; Bento-Silva, A.; Serra, A.T.; Mena, P.; Legua, P.; Bronze, M.R. Phytochemical Profile of *Opuntia ficus-indica* (L.) Mill Fruits (Cv.'Orito') Stored at Different Conditions. *Foods* **2022**, *11*, 160. [CrossRef] [PubMed]
51. Butera, D.; Tesoriere, L.; Di Gaudio, F.; Bongiorno, A.; Allegra, M.; Pintaudi, A.M.; Kohen, R.; Livrea, M.A. Antioxidant Activities of Sicilian Prickly Pear (*Opuntia ficus indica*) Fruit Extracts and Reducing Properties of Its Betalains: Betanin and Indicaxanthin. *J. Agric. Food Chem.* **2002**, *50*, 6895–6901. [CrossRef] [PubMed]
52. Zeghbib, W.; Boudjouan, F.; Vasconcelos, V.; Lopes, G. Phenolic Compounds' Occurrence in *Opuntia* Species and Their Role in the Inflammatory Process: A Review. *Molecules* **2022**, *27*, 4763. [CrossRef] [PubMed]
53. Antunes-Ricardo, M.; Rodríguez-Rodríguez, C.; Gutiérrez-Uribe, J.A.; Cepeda-Cañedo, E.; Serna-Saldívar, S.O. Bioaccessibility, Intestinal Permeability and Plasma Stability of Isorhamnetin Glycosides from *Opuntia ficus-indica* (L.). *Int. J. Mol. Sci.* **2017**, *18*, 1816. [CrossRef]
54. Alexandre, E.M.; Coelho, M.C.; Ozcan, K.; Pinto, C.A.; Teixeira, J.A.; Saraiva, J.A.; Pintado, M. Emergent Technologies for the Extraction of Antioxidants from Prickly Pear Peel and Their Antimicrobial Activity. *Foods* **2021**, *10*, 570. [CrossRef]
55. Albano, C.; Negro, C.; Tommasi, N.; Gerardi, C.; Mita, G.; Miceli, A.; De Bellis, L.; Blando, F. Betalains, Phenols and Antioxidant Capacity in Cactus Pear [*Opuntia ficus-indica* (L.) Mill.] Fruits from Apulia (South Italy) Genotypes. *Antioxidants* **2015**, *4*, 269–280. [CrossRef]
56. Xu, J.; Yan, J.; Li, W.; Wang, Q.; Wang, C.; Guo, J.; Geng, D.; Guan, Q.; Ma, F. Integrative Analyses of Widely Targeted Metabolic Profiling and Transcriptome Data Reveals Molecular Insight into Metabolomic Variations during Apple (*Malus domestica*) Fruit Development and Ripening. *Int. J. Mol. Sci.* **2020**, *21*, 4797. [CrossRef]
57. Seong, G.-U.; Yun, D.-Y.; Cho, J.-S.; Park, S.-K.; Lee, G.S.; Choi, J.H.; Park, K.-J.; Lim, J.-H. Ripening-related Metabolic Changes in Different Chili Pepper Cultivars Revealed by Nuclear Magnetic Resonance Spectroscopy. *J. Sci. Food Agric.* **2025**, *105*, 6084–6093. [CrossRef]
58. Slámová, K.; Kapešová, J.; Valentová, K. "Sweet Flavonoids": Glycosidase-Catalyzed Modifications. *Int. J. Mol. Sci.* **2018**, *19*, 2126. [CrossRef]
59. Liu, S.; Li, D.; Qin, Z.; Zeng, W.; Zhou, J. Enhancing Glycosylation of Flavonoids by Engineering the Uridine Diphosphate Glucose Supply in *Escherichia coli*. *J. Agric. Food Chem.* **2023**, *71*, 17842–17851. [CrossRef]
60. Le Roy, J.; Huss, B.; Creach, A.; Hawkins, S.; Neutelings, G. Glycosylation Is a Major Regulator of Phenylpropanoid Availability and Biological Activity in Plants. *Front. Plant Sci.* **2016**, *7*, 735. [CrossRef] [PubMed]
61. Plaza, M.; Pozzo, T.; Liu, J.; Gulshan Ara, K.Z.; Turner, C.; Nordberg Karlsson, E. Substituent Effects on in Vitro Antioxidizing Properties, Stability, and Solubility in Flavonoids. *J. Agric. Food Chem.* **2014**, *62*, 3321–3333. [CrossRef] [PubMed]
62. Ji, Y.; Li, B.; Qiao, M.; Li, J.; Xu, H.; Zhang, L.; Zhang, X. Advances on the in Vivo and in Vitro Glycosylations of Flavonoids. *Appl. Microbiol. Biotechnol.* **2020**, *104*, 6587–6600. [CrossRef] [PubMed]
63. Sun, W.; Liang, L.; Meng, X.; Li, Y.; Gao, F.; Liu, X.; Wang, S.; Gao, X.; Wang, L. Biochemical and Molecular Characterization of a Flavonoid 3-O-Glycosyltransferase Responsible for Anthocyanins and Flavonols Biosynthesis in Freesia Hybrida. *Front. Plant Sci.* **2016**, *7*, 410. [CrossRef] [PubMed]
64. Filimonov, D.A.; Lagunin, A.A.; Gloriozova, T.A.; Rudik, A.V.; Druzhilovskii, D.S.; Pogodin, P.V.; Poroikov, V.V. Prediction of the Biological Activity Spectra of Organic Compounds Using the PASS Online Web Resource. *Chem. Heterocycl. Compd.* **2014**, *50*, 444–457. [CrossRef]

65. Lagunin, A.; Filimonov, D.; Poroikov, V. Multi-Targeted Natural Products Evaluation Based on Biological Activity Prediction with PASS. *Curr. Pharm. Des.* **2010**, *16*, 1703–1717. [CrossRef]
66. Olaokun, O.O. Computational Identification of Polyphenols from Medicinal Plant Extracts with Biological Activity against Oxidative Stress-Related Diseases: An in Silico Anti-Inflammatory Study. *S. Afr. J. Bot.* **2025**, *183*, 62–73. [CrossRef]
67. Lagunin, A.; Stepanchikova, A.; Filimonov, D.; Poroikov, V. PASS: Prediction of Activity Spectra for Biologically Active Substances. *Bioinformatics* **2000**, *16*, 747–748. [CrossRef]
68. Antunes-Ricardo, M.; Gutiérrez-Uribe, J.A.; López-Pacheco, F.; Alvarez, M.M.; Serna-Saldívar, S.O. In Vivo Anti-Inflammatory Effects of Isorhamnetin Glycosides Isolated from *Opuntia ficus-indica* (L.) Mill Cladodes. *Ind. Crops Prod.* **2015**, *76*, 803–808. [CrossRef]
69. Fakhri, S.; Abbaszadeh, F.; Moradi, S.Z.; Cao, H.; Khan, H.; Xiao, J. Effects of Polyphenols on Oxidative Stress, Inflammation, and Interconnected Pathways during Spinal Cord Injury. *Oxidative Med. Cell. Longev.* **2022**, *2022*, 8100195. [CrossRef]
70. Gomes, A.; Fernandes, E.; Lima, J.L.; Mira, L.; Corvo, M.L. Molecular Mechanisms of Anti-Inflammatory Activity Mediated by Flavonoids. *Curr. Med. Chem.* **2008**, *15*, 1586–1605. [CrossRef]
71. Marhri, A.; Rbah, Y.; Allay, A.; Boumediene, M.; Tikent, A.; Benmoumen, A.; Melhaoui, R.; Elamrani, A.; Abid, M.; Addi, M. Comparative Analysis of Antioxidant Potency and Phenolic Compounds in Fruit Peel of Opuntia Robusta, Opuntia Dillenii, and *Opuntia ficus-indica* Using HPLC-DAD Profiling. *J. Food Qual.* **2024**, *2024*, 2742606. [CrossRef]
72. Monter-Arciniega, A.; Hernández-Falcón, T.A.; Cruz-Cansino, N.d.S.; Ramírez-Moreno, E.; Alanís-García, E.; Arias-Rico, J.; Ariza-Ortega, J.A. Functional Properties, Total Phenolic Content and Antioxidant Activity of Purple Cactus Pear (*Opuntia ficus-indica*) Waste: Comparison with Commercial Fibers. *Waste Biomass Valorization* **2019**, *10*, 2897–2906. [CrossRef]
73. Zeghbib, W.; Boudjouan, F.; Carneiro, J.; Oliveira, A.L.; Sousa, S.F.; Pintado, M.E.; Ourabah, A.; Vasconcelos, V.; Lopes, G. LC-ESI-UHR-QqTOF-MS/MS Profiling and Anti-Inflammatory Potential of the Cultivated *Opuntia ficus-indica* (L.) Mill. and the Wild *Opuntia stricta* (Haw.) Haw. Fruits from the Algerian Region. *Food Chem.* **2024**, *460*, 140414. [CrossRef] [PubMed]
74. Melgar, B.; Dias, M.I.; Ciric, A.; Sokovic, M.; Garcia-Castello, E.M.; Rodriguez-Lopez, A.D.; Barros, L.; Ferreira, I. By-Product Recovery of *Opuntia* spp. Peels: Betalainic and Phenolic Profiles and Bioactive Properties. *Ind. Crops Prod.* **2017**, *107*, 353–359. [CrossRef]
75. Modarresi Chahardehi, A.; Arsad, H.; Lim, V. Zebrafish as a Successful Animal Model for Screening Toxicity of Medicinal Plants. *Plants* **2020**, *9*, 1345. [CrossRef]
76. Bauer, B.; Mally, A.; Liedtke, D. Zebrafish Embryos and Larvae as Alternative Animal Models for Toxicity Testing. *Int. J. Mol. Sci.* **2021**, *22*, 13417. [CrossRef] [PubMed]
77. Hassoun, E.; Kariya, C.; Williams, F.E. Dichloroacetate-induced Developmental Toxicity and Production of Reactive Oxygen Species in Zebrafish Embryos. *J. Biochem. Mol. Toxicol.* **2005**, *19*, 52–58. [CrossRef]
78. Alafiatayo, A.A.; Lai, K.-S.; Syahida, A.; Mahmood, M.; Shaharuddin, N.A. Phytochemical Evaluation, Embryotoxicity, and Teratogenic Effects of Curcuma Longa Extract on Zebrafish (*Danio rerio*). *Evid.-Based Complement. Altern. Med.* **2019**, *2019*, 3807207.
79. Pagliari, S.; Sicari, M.; Pansera, L.; Guidi Nissim, W.; Mhalhel, K.; Rastegar, S.; Germanà, A.; Cicero, N.; Labra, M.; Cannavacciuolo, C. A Comparative Metabolomic Investigation of Different Sections of Sicilian *Citrus* x *Limon* (L.) Osbeck, Characterization of Bioactive Metabolites, and Evaluation of in Vivo Toxicity on Zebrafish Embryo. *J. Food Sci.* **2024**, *89*, 3729–3744. [CrossRef]
80. Ahmad, F. *Zebrafish Embryos and Larvae as a Complementary Model for Behavioural Research*; Universiteit Leiden: Leiden, The Netherlands, 2014.
81. Sicari, M.; Pansera, L.; Mhalhel, K.; Aragona, M.; Galeano, M.; Colonna, M.R.; Levanti, M.; Laurà, R.; Abbate, F.; Germanà, A.; et al. Evaluation of Polyphenol-Rich Lemon Peel Extract Use in a Zebrafish Model of Spinal Cord Injury: Morphology, Repair-Associated Markers, and Inflammatory Profile. *Int. J. Mol. Sci.* **2026**, *27*, 1201. [CrossRef]
82. Komorowska, W.; Kurach, Ł.; Dąbrowska, A. Nanopolystyrene (nanoPS) and Sodium Azide (NaN_3) Toxicity in *Danio rerio*: Behavioural and Morphological Evaluation. *Microplastics* **2025**, *4*, 45. [CrossRef]
83. Cigliola, V.; Shoffner, A.; Lee, N.; Ou, J.; Gonzalez, T.J.; Hoque, J.; Becker, C.J.; Han, Y.; Shen, G.; Faw, T.D. Spinal Cord Repair Is Modulated by the Neurogenic Factor Hb-Egf under Direction of a Regeneration-Associated Enhancer. *Nat. Commun.* **2023**, *14*, 4857. [CrossRef]
84. Hossainian, D.; Shao, E.; Jiao, B.; Ilin, V.A.; Parris, R.S.; Zhou, Y.; Bai, Q.; Burton, E.A. Quantification of Functional Recovery in a Larval Zebrafish Model of Spinal Cord Injury. *J. Neurosci. Res.* **2022**, *100*, 2044–2054. [CrossRef]
85. Tsata, V.; Möllmert, S.; Schweitzer, C.; Kolb, J.; Möckel, C.; Böhm, B.; Rosso, G.; Lange, C.; Lesche, M.; Hammer, J. A Switch in Pdgfrb+ Cell-Derived ECM Composition Prevents Inhibitory Scarring and Promotes Axon Regeneration in the Zebrafish Spinal Cord. *Dev. Cell* **2021**, *56*, 509–524. [CrossRef] [PubMed]
86. Kaka, G.; Yaghoobi, K.; Davoodi, S.; Hosseini, S.R.; Sadraie, S.H.; Mansouri, K. Assessment of the Neuroprotective Effects of *Lavandula angustifolia* Extract on the Contusive Model of Spinal Cord Injury in Wistar Rats. *Front. Neurosci.* **2016**, *10*, 25. [CrossRef] [PubMed]

87. Feng, S.; Liu, L.; Cheng, Y.; Zhou, M.; Zhu, H.; Zhao, X.; Chen, Z.; Kan, S.; Fu, X.; Hu, W. Icariin Promotes Functional Recovery in Rats after Spinal Cord Injury by Inhibiting YAP and Regulating PPM1B Ubiquitination to Inhibiting the Activation of Reactive Astrocytes. *Front. Pharmacol.* **2024**, *15*, 1434652, Erratum in *Front. Pharmacol*. **2024**, *15*, 1523605..
88. de Oliveira, S.; Reyes-Aldasoro, C.C.; Candel, S.; Renshaw, S.A.; Mulero, V.; Calado, A. Cxcl8 (IL-8) Mediates Neutrophil Recruitment and Behavior in the Zebrafish Inflammatory Response. *J. Immunol.* **2013**, *190*, 4349–4359. [CrossRef]
89. Tsarouchas, T.M.; Wehner, D.; Cavone, L.; Munir, T.; Keatinge, M.; Lambertus, M.; Underhill, A.; Barrett, T.; Kassapis, E.; Ogryzko, N.; et al. Dynamic Control of Proinflammatory Cytokines Il-1β and Tnf-α by Macrophages in Zebrafish Spinal Cord Regeneration. *Nat. Commun.* **2018**, *9*, 4670. [CrossRef] [PubMed]
90. Li, H.; Zhang, X.; Zhu, X.; Qi, X.; Lin, K.; Cheng, L. The Effects of Icariin on Enhancing Motor Recovery through Attenuating Pro-Inflammatory Factors and Oxidative Stress via Mitochondrial Apoptotic Pathway in the Mice Model of Spinal Cord Injury. *Front. Physiol.* **2018**, *9*, 1617. [CrossRef]
91. Besné-Eseverri, I.; Martín, M.Á.; Lobo, G.; Cano, M.P.; Portillo, M.P.; Trepiana, J. Antioxidant and Anti-Inflammatory Effects of Opuntia Extracts on a Model of Diet-Induced Steatosis. *Antioxidants* **2024**, *13*, 1416. [CrossRef]
92. Chaalal, M.; Louaileche, H.; Touati, N.; Bey, M.B. Phytochemicals, in Vitro Antioxidant Capacity and Antiradical Potential of Whole and Ground Seeds of Three Prickly Pear Varieties: A Comparative Study. *Ind. Crops Prod.* **2013**, *49*, 386–391. [CrossRef]
93. Ammar, I.; Salem, M.B.; Harrabi, B.; Mzid, M.; Bardaa, S.; Sahnoun, Z.; Attia, H.; Ennouri, M. Anti-Inflammatory Activity and Phenolic Composition of Prickly Pear (*Opuntia ficus-indica*) Flowers. *Ind. Crops Prod.* **2018**, *112*, 313–319. [CrossRef]
94. Muvhulawa, N.; Dludla, P.V.; Ziqubu, K.; Mthembu, S.X.; Mthiyane, F.; Nkambule, B.B.; Mazibuko-Mbeje, S.E. Rutin Ameliorates Inflammation and Improves Metabolic Function: A Comprehensive Analysis of Scientific Literature. *Pharmacol. Res.* **2022**, *178*, 106163. [CrossRef]
95. Song, H.; Zhang, X.; Wang, W.; Liu, R.; Zhao, K.; Liu, M.; Gong, W.; Ning, B. Neuroprotective Mechanisms of Rutin for Spinal Cord Injury through Anti-Oxidation and Anti-Inflammation and Inhibition of P38 Mitogen Activated Protein Kinase Pathway. *Neural Regen. Res.* **2018**, *13*, 128–134. [PubMed]
96. Özbek, Z.; Aydin, H.; Kocman, A.; Özkara, E.; Şahin, E.; Bektur, E.; Vural, M.; Köse, A.; Arslantaş, A.; Baycu, C. Neuroprotective Effect of Genistein in Peripheral Nerve Injury. *Turk. Neurosurg.* **2017**, *27*, 816–822. [PubMed]
97. Germanà, A.; Guerrera, M.C.; Laurà, R.; Levanti, M.; Aragona, M.; Mhalhel, K.; Germanà, G.; Montalbano, G.; Abbate, F. Expression and Localization of BDNF/TrkB System in the Zebrafish Inner Ear. *Int. J. Mol. Sci.* **2020**, *21*, 5787. [CrossRef]
98. Gustafsson, D.; Klang, A.; Thams, S.; Rostami, E. The Role of BDNF in Experimental and Clinical Traumatic Brain Injury. *Int. J. Mol. Sci.* **2021**, *22*, 3582. [CrossRef]
99. Houlton, J.; Abumaria, N.; Hinkley, S.F.R.; Clarkson, A.N. Therapeutic Potential of Neurotrophins for Repair After Brain Injury: A Helping Hand from Biomaterials. *Front. Neurosci.* **2019**, *13*, 790. [CrossRef]
100. Aragona, M.; Mhalhel, K.; Pansera, L.; Montalbano, G.; Guerrera, M.C.; Levanti, M.; Laurà, R.; Abbate, F.; Vega, J.A.; Germanà, A. Localization of Piezo 1 and Piezo 2 in Lateral Line System and Inner Ear of Zebrafish (*Danio rerio*). *Int. J. Mol. Sci.* **2024**, *25*, 9204. [CrossRef]
101. Aragona, M.; Porcino, C.; Guerrera, M.C.; Montalbano, G.; Laurà, R.; Cometa, M.; Levanti, M.; Abbate, F.; Cobo, T.; Capitelli, G. The BDNF/TrkB Neurotrophin System in the Sensory Organs of Zebrafish. *Int. J. Mol. Sci.* **2022**, *23*, 2621. [CrossRef] [PubMed]
102. Aragona, M.; Porcino, C.; Guerrera, M.C.; Montalbano, G.; Laurà, R.; Levanti, M.; Abbate, F.; Cobo, T.; Capitelli, G.; Calapai, F.; et al. Localization of BDNF and Calretinin in Olfactory Epithelium and Taste Buds of Zebrafish (*Danio rerio*). *Int. J. Mol. Sci.* **2022**, *23*, 4696. [CrossRef]
103. Kowiański, P.; Lietzau, G.; Czuba, E.; Waśkow, M.; Steliga, A.; Moryś, J. BDNF: A Key Factor with Multipotent Impact on Brain Signaling and Synaptic Plasticity. *Cell. Mol. Neurobiol.* **2018**, *38*, 579–593. [CrossRef] [PubMed]
104. DePaul, M.A.; Lin, C.-Y.; Silver, J.; Lee, Y.-S. Combinatory Repair Strategy to Promote Axon Regeneration and Functional Recovery after Chronic Spinal Cord Injury. *Sci. Rep.* **2017**, *7*, 9018. [CrossRef] [PubMed]
105. Zeng, C.-W. Macrophage–Neuroglia Interactions in Promoting Neuronal Regeneration in Zebrafish. *Int. J. Mol. Sci.* **2023**, *24*, 6483. [CrossRef]
106. Assuncao Silva, R.C.; Pinto, L.; Salgado, A.J. Cell Transplantation and Secretome Based Approaches in Spinal Cord Injury Regenerative Medicine. *Med. Res. Rev.* **2022**, *42*, 850–896. [CrossRef]
107. Feng, Y.; Li, Y.; Shen, P.-P.; Wang, B. Gene-Modified Stem Cells for Spinal Cord Injury: A Promising Better Alternative Therapy. *Stem Cell Rev. Rep.* **2022**, *18*, 2662–2682. [CrossRef]
108. Cacialli, P.; Ricci, S.; Lazzari, M.; Milani, L.; Franceschini, V. Transcription Pattern of Neurotrophic Factors and Their Receptors in Adult Zebrafish Spinal Cord. *Int. J. Mol. Sci.* **2023**, *24*, 10953. [CrossRef]
109. Namiki, J.U.N.; Kojima, A.; Tator, C.H. Effect of Brain-Derived Neurotrophic Factor, Nerve Growth Factor, and Neurotrophin-3 on Functional Recovery and Regeneration after Spinal Cord Injury in Adult Rats. *J. Neurotrauma* **2000**, *17*, 1219–1231. [CrossRef] [PubMed]

110. Cacialli, P.; D'angelo, L.; Kah, O.; Coumailleau, P.; Gueguen, M.; Pellegrini, E.; Lucini, C. Neuronal Expression of Brain Derived Neurotrophic Factor in the Injured Telencephalon of Adult Zebrafish. *J. Comp. Neurol.* **2018**, *526*, 569–582. [CrossRef] [PubMed]
111. Cellini, B.R.; Edachola, S.V.; Faw, T.D.; Cigliola, V. Blueprints for Healing: Central Nervous System Regeneration in Zebrafish and Neonatal Mice. *BMC Biol.* **2025**, *23*, 115. [CrossRef]
112. Park, S.E.; Sapkota, K.; Kim, S.; Kim, H.; Kim, S.J. Kaempferol Acts through Mitogen-activated Protein Kinases and Protein Kinase B/AKT to Elicit Protection in a Model of Neuroinflammation in BV2 Microglial Cells. *Br. J. Pharmacol.* **2011**, *164*, 1008–1025. [CrossRef]
113. Yao, R.-Q.; Qi, D.-S.; Yu, H.-L.; Liu, J.; Yang, L.-H.; Wu, X.-X. Quercetin Attenuates Cell Apoptosis in Focal Cerebral Ischemia Rat Brain via Activation of BDNF–TrkB–PI3K/Akt Signaling Pathway. *Neurochem. Res.* **2012**, *37*, 2777–2786. [CrossRef] [PubMed]
114. Karar, J.; Maity, A. PI3K/AKT/mTOR Pathway in Angiogenesis. *Front. Mol. Neurosci.* **2011**, *4*, 51. [CrossRef] [PubMed]
115. Franke, T.F.; Hornik, C.P.; Segev, L.; Shostak, G.A.; Sugimoto, C. PI3K/Akt and Apoptosis: Size Matters. *Oncogene* **2003**, *22*, 8983–8998. [CrossRef]
116. Xiao, C.-L.; Yin, W.-C.; Zhong, Y.-C.; Luo, J.-Q.; Liu, L.-L.; Liu, W.-Y.; Zhao, K. The Role of PI3K/Akt Signalling Pathway in Spinal Cord Injury. *Biomed. Pharmacother.* **2022**, *156*, 113881. [CrossRef]
117. Wu, J.; He, J.; Tian, X.; Zhong, J.; Li, H.; Sun, X. Activation of the Hedgehog Pathway Promotes Recovery of Neurological Function after Traumatic Brain Injury by Protecting the Neurovascular Unit. *Transl. Stroke Res.* **2020**, *11*, 720–733. [CrossRef]
118. Williams, J.A. Hedgehog and Spinal Cord Injury. *Expert Opin. Ther. Targets* **2005**, *9*, 1137–1145. [CrossRef]
119. Machold, R.; Fishell, G. Hedgehog Patterns Midbrain ARChitecture. *Trends Neurosci.* **2002**, *25*, 10–11. [CrossRef]
120. Prajapati, A.; Mehan, S.; Khan, Z. The Role of Smo-Shh/Gli Signaling Activation in the Prevention of Neurological and Ageing Disorders. *Biogerontology* **2023**, *24*, 493–531, Erratum in *Biogerontology* **2023**, *24*, 829. [CrossRef]
121. Choudhry, Z.; Rikani, A.A.; Choudhry, A.M.; Tariq, S.; Zakaria, F.; Asghar, M.W.; Sarfraz, M.K.; Haider, K.; Shafiq, A.A.; Mobassarah, N.J. Sonic Hedgehog Signalling Pathway: A Complex Network. *Ann. Neurosci.* **2014**, *21*, 28. [CrossRef]
122. Teraoka, H.; Russell, C.; Regan, J.; Chandrasekhar, A.; Concha, M.L.; Yokoyama, R.; Higashi, K.; Take-Uchi, M.; Dong, W.; Hiraga, T. Hedgehog and Fgf Signaling Pathways Regulate the Development of tphR-expressing Serotonergic Raphe Neurons in Zebrafish Embryos. *J. Neurobiol.* **2004**, *60*, 275–288. [CrossRef] [PubMed]
123. Echelard, Y.; Epstein, D.J.; St-Jacques, B.; Shen, L.; Mohler, J.; McMahon, J.A.; McMahon, A.P. Sonic Hedgehog, a Member of a Family of Putative Signaling Molecules, Is Implicated in the Regulation of CNS Polarity. *Cell* **1993**, *75*, 1417–1430. [CrossRef]
124. So, P.-L.; Yip, P.K.; Bunting, S.; Wong, L.-F.; Mazarakis, N.D.; Hall, S.; McMahon, S.; Maden, M.; Corcoran, J.P. Interactions between Retinoic Acid, Nerve Growth Factor and Sonic Hedgehog Signalling Pathways in Neurite Outgrowth. *Dev. Biol.* **2006**, *298*, 167–175. [CrossRef]
125. Lowry, N.; Goderie, S.K.; Lederman, P.; Charniga, C.; Gooch, M.R.; Gracey, K.D.; Banerjee, A.; Punyani, S.; Silver, J.; Kane, R.S. The Effect of Long-Term Release of Shh from Implanted Biodegradable Microspheres on Recovery from Spinal Cord Injury in Mice. *Biomaterials* **2012**, *33*, 2892–2901. [CrossRef]
126. Dai, R.-L.; Zhu, S.-Y.; Xia, Y.-P.; Mao, L.; Mei, Y.-W.; Yao, Y.-F.; Xue, Y.-M.; Hu, B. Sonic Hedgehog Protects Cortical Neurons against Oxidative Stress. *Neurochem. Res.* **2011**, *36*, 67–75. [CrossRef]
127. Salybekov, A.A.; Salybekova, A.K.; Pola, R.; Asahara, T. Sonic Hedgehog Signaling Pathway in Endothelial Progenitor Cell Biology for Vascular Medicine. *Int. J. Mol. Sci.* **2018**, *19*, 3040. [CrossRef] [PubMed]
128. Ferent, J.; Traiffort, E. Hedgehog: Multiple Paths for Multiple Roles in Shaping the Brain and Spinal Cord. *Neuroscientist* **2015**, *21*, 356–371. [CrossRef] [PubMed]
129. Cawsey, T.; Duflou, J.; Weickert, C.S.; Gorrie, C.A. Nestin-Positive Ependymal Cells Are Increased in the Human Spinal Cord after Traumatic Central Nervous System Injury. *J. Neurotrauma* **2015**, *32*, 1393–1402. [CrossRef] [PubMed]
130. Shibuya, S.; Miyamoto, O.; Auer, R.N.; Itano, T.; Mori, S.; Norimatsu, H. Embryonic Intermediate Filament, Nestin, Expression Following Traumatic Spinal Cord Injury in Adult Rats. *Neuroscience* **2002**, *114*, 905–916. [CrossRef]
131. Ceci, M.; Mariano, V.; Romano, N. Zebrafish as a Translational Regeneration Model to Study the Activation of Neural Stem Cells and Role of Their Environment. *Rev. Neurosci.* **2019**, *30*, 45–66. [CrossRef]
132. Zhang, P.; Hölscher, C.; Ma, X. Therapeutic Potential of Flavonoids in Spinal Cord Injury. *Rev. Neurosci.* **2017**, *28*, 87–101. [CrossRef] [PubMed]
133. Zhang, G.; Lübke, L.; Chen, F.; Beil, T.; Takamiya, M.; Diotel, N.; Strähle, U.; Rastegar, S. Neuron-Radial Glial Cell Communication via BMP/Id1 Signaling Is Key to Long-Term Maintenance of the Regenerative Capacity of the Adult Zebrafish Telencephalon. *Cells* **2021**, *10*, 2794. [CrossRef]
134. Fakhri, S.; Gravandi, M.M.; Abdian, S.; Moradi, S.Z.; Echeverría, J. Quercetin Derivatives in Combating Spinal Cord Injury: A Mechanistic and Systematic Review. *Life* **2022**, *12*, 1960. [CrossRef] [PubMed]
135. Schültke, E.; Kendall, E.; Kamencic, H.; Ghong, Z.; Griebel, R.W.; Juurlink, B.H.J. Quercetin Promotes Functional Recovery Following Acute Spinal Cord Injury. *J. Neurotrauma* **2003**, *20*, 583–591. [CrossRef] [PubMed]

136. Cannavacciuolo, C.; Pagliari, S.; Giustra, C.M.; Carabetta, S.; Guidi Nissim, W.; Russo, M.; Branduardi, P.; Labra, M.; Campone, L. LC-MS and GC-MS Data Fusion Metabolomics Profiling Coupled with Multivariate Analysis for the Discrimination of Different Parts of Faustrime Fruit and Evaluation of Their Antioxidant Activity. *Antioxidants* **2023**, *12*, 565. [CrossRef]
137. OECD. *OECD Guidelines for the Testing of Chemicals, Section 2 Test No. 236: Fish Embryo Acute Toxicity (FET) Test*; OECD: Paris, UK, 2013; Volume 2, pp. 1–22.
138. Slob, W. Dose-Response Modeling of Continuous Endpoints. *Toxicol. Sci.* **2002**, *66*, 298–312. [CrossRef] [PubMed]
139. Oprişoreanu, A.-M.; Ryan, F.; Richmond, C.; Dzekhtsiarova, Y.; Carragher, N.O.; Becker, T.; David, S.; Becker, C.G. Drug Screening in Zebrafish Larvae Reveals Inflammation-Related Modulators of Secondary Damage after Spinal Cord Injury in Mice. *Theranostics* **2023**, *13*, 2531. [CrossRef]
140. Bustin, S.A.; Benes, V.; Garson, J.A.; Hellemans, J.; Huggett, J.; Kubista, M.; Mueller, R.; Nolan, T.; Pfaffl, M.W.; Shipley, G.L. *The MIQE Guidelines: Minimum Information for Publication of Quantitative Real-Time PCR Experiments*; Oxford University Press: Oxford, UK, 2009.
141. Mhalhel, K.; Germanà, A.; Abbate, F.; Guerrera, M.C.; Levanti, M.; Laurà, R.; Montalbano, G. The Effect of Orally Supplemented Melatonin on Larval Performance and Skeletal Deformities in Farmed Gilthead Seabream (*Sparus aurata*). *Int. J. Mol. Sci.* **2020**, *21*, 9597. [CrossRef]
142. Mhalhel, K.; Briglia, M.; Aragona, M.; Porcino, C.; Abbate, F.; Guerrera, M.C.; Laurà, R.; Krichen, Y.; Guerbej, H.; Germanà, A.; et al. Nothobranchius as a Model for Anorexia of Aging Research: An Evolutionary, Anatomical, Histological, Immunohistochemical, and Molecular Study. *Ann. Anat.-Anat. Anz.* **2023**, *250*, 152116. [CrossRef]
143. Ye, J.; Coulouris, G.; Zaretskaya, I.; Cutcutache, I.; Rozen, S.; Madden, T.L. Primer-BLAST: A Tool to Design Target-Specific Primers for Polymerase Chain Reaction. *BMC Bioinform.* **2012**, *13*, 134. [CrossRef]
144. Mhalhel, K.; Cavallaro, M.; Pansera, L.; Ledesma, L.H.; Levanti, M.; Germanà, A.; Sutera, A.M.; Tardiolo, G.; Zumbo, A.; Aragona, M.; et al. Histological Assessment of Intestinal Changes Induced by Liquid Whey-Enriched Diets in Pigs. *Vet. Sci.* **2025**, *12*, 716. [CrossRef]